Impacts of Climate Change on the Ascension Island Marine Protected Area and its ecosystem services

Lee de Mora[1], Giovannni Galli[1], Yuri Artioli[1], Stefanie Broszeit[1], Diane Baum[2], Sam Weber[3], and Jerry Blackford[1]

[1]Plymouth Marine Laboratory
[2]Ascension Island Government
[3]University of Exeter

January 20, 2023

Abstract

This is the first forecast of marine circulation and biogeochemistry for the Ascension Island Marine Protected Area (MPA). MPAs are a key management tools used to safeguard ocean biodiversity from human impacts, but their efficacy is increasingly threatened by anthropogenic climate change. To assess the vulnerability of individual MPAs to climate change and predict biological responses, it is first necessary to forecast how local marine environments will change. We found that the MPA will become warmer, more saline, more acidic, with less nutrients, less chlorophyll and less primary production by the mid-century. A weakening of the Atlantic equatorial undercurrent is forecast in all scenarios. In most cases, these changes are more extreme in the scenarios with higher greenhouse gases emissions and more significant climate change. The mean rise in temperature is between 0.9 \degree C and 1.2 \degree C over the first half of the 21st century. The integrated primary production and nutrients are forecast to decline in the MPA, but there is less consistency between models in projections of salinity, surface chlorophyll, and dissolved oxygen concentration at 500m depth. The combined effects of these projections may lead to changes in ecosystem services around Ascension Island. The effects of the model outputs were interpreted for three key ecosystem service providing habitats: biogenic deep sea habitats, intertidal sand and intertidal rocky shores. The outcomes were then used to assess potential effects on eight marine and coastal ecosystem services and information was compared to current ecosystem service levels.

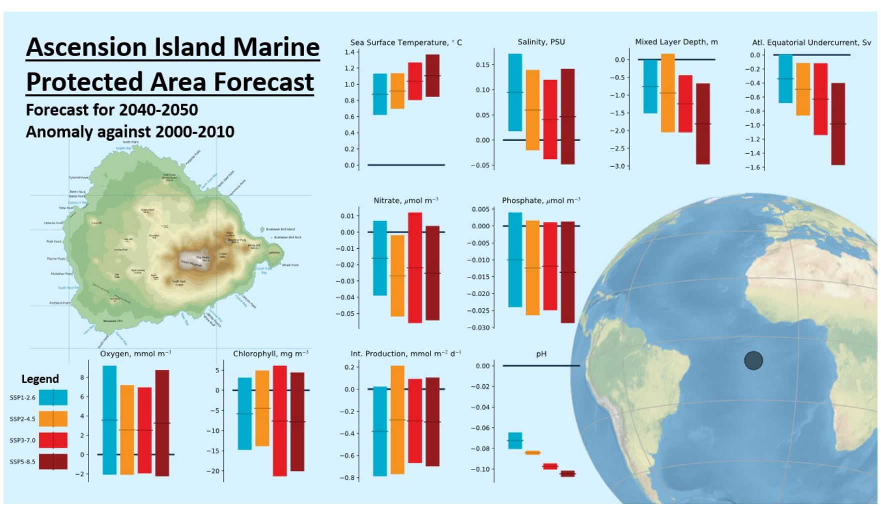

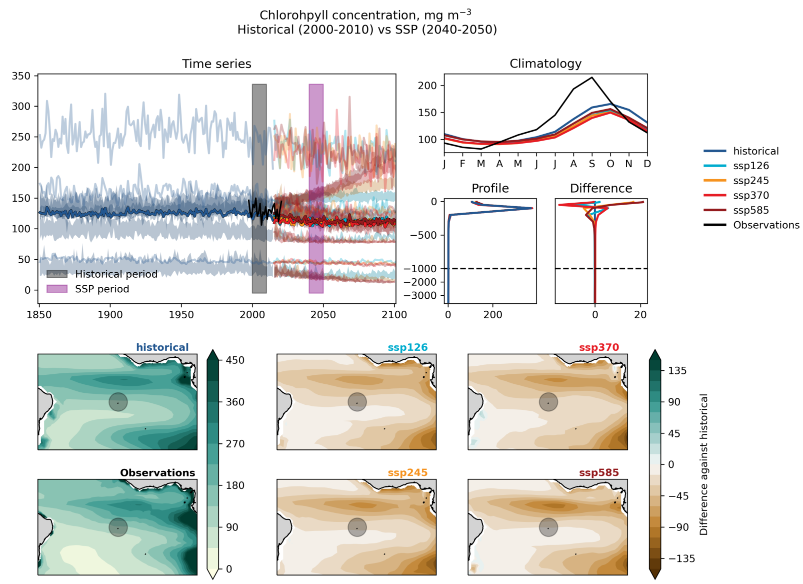
Chlorohpyll concentration, mg m^{-3}
Historical (2000-2010) vs SSP (2040-2050)
Time series
Climatology
Profile
Difference
Historical period
SSP period
historical
ssp126
ssp245
ssp370
ssp585
Observations
Difference against historical

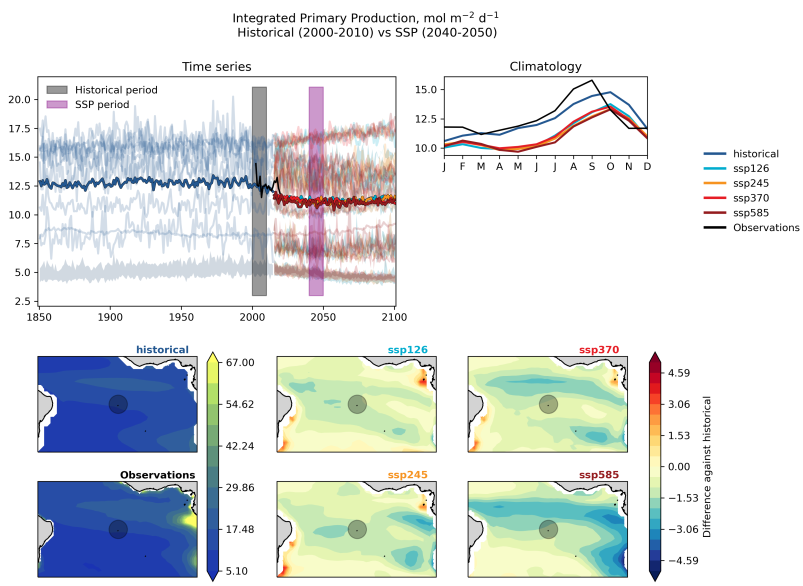
Integrated Primary Production, mol m^{-2} d^{-1}
Historical (2000-2010) vs SSP (2040-2050)
Time series
Climatology
Historical period
SSP period
historical
ssp126
ssp245
ssp370
ssp585
Observations
Difference against historical

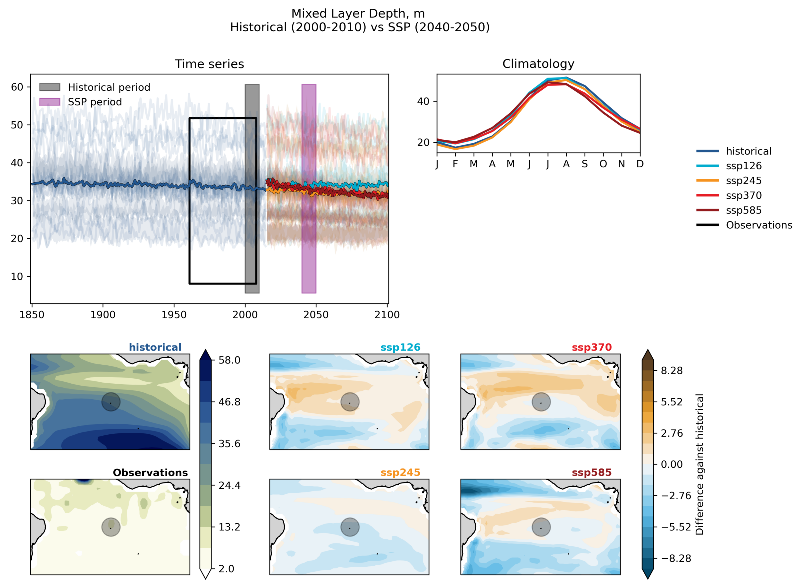
Mixed Layer Depth, m
Historical (2000-2010) vs SSP (2040-2050)
Time series
Historical period
SSP period
Climatology
historical
ssp126
ssp245
ssp370
ssp585
Observations
historical
Observations
ssp126
ssp245
ssp370
ssp585
Difference against historical

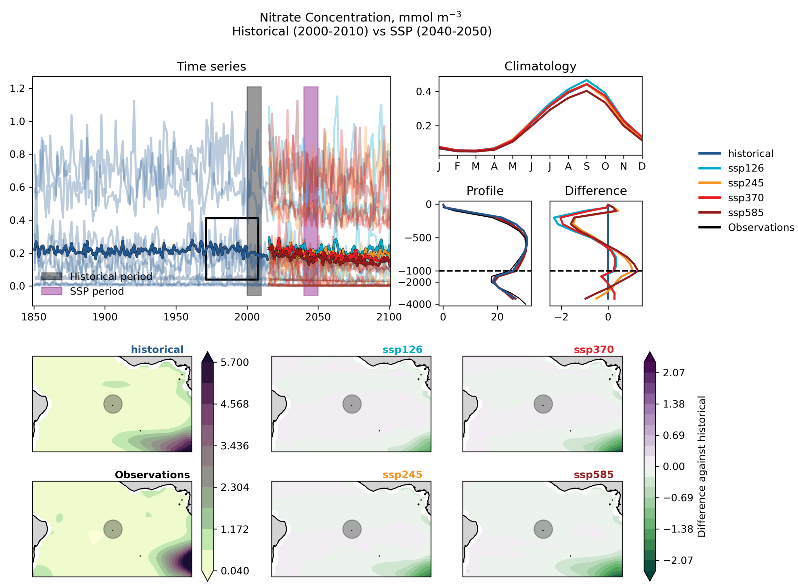
Nitrate Concentration, mmol m^{-3}
Historical (2000-2010) vs SSP (2040-2050)
Time series
Historical period
SSP period
Climatology
Profile
Difference
historical
ssp126
ssp245
ssp370
ssp585
Observations
historical
Observations
ssp126
ssp245
ssp370
ssp585
Difference against historical

Disolved Oxygen Concentration at 500m, mmol m^{-3}
Historical (2000-2010) vs SSP (2040-2050)

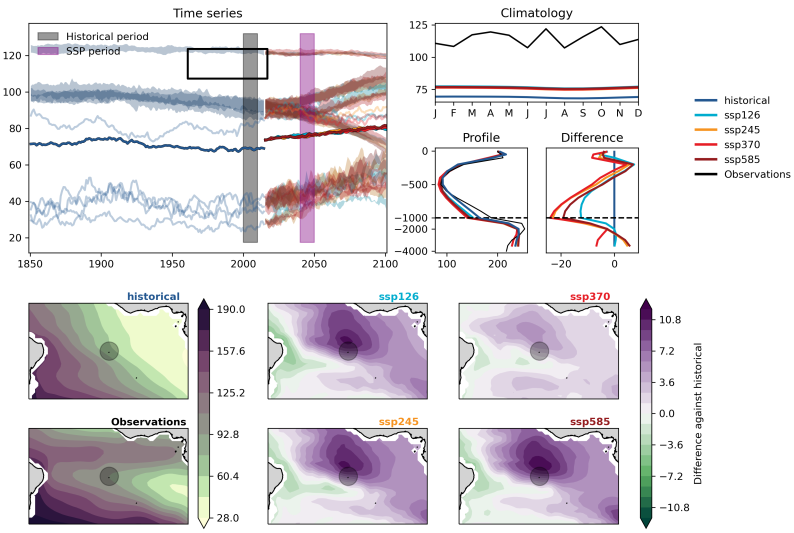

pH
Historical (2000-2010) vs SSP (2040-2050)

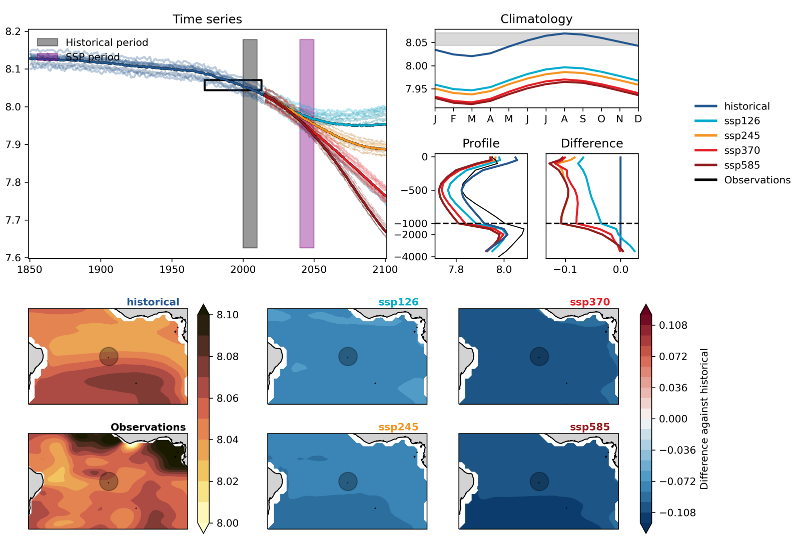

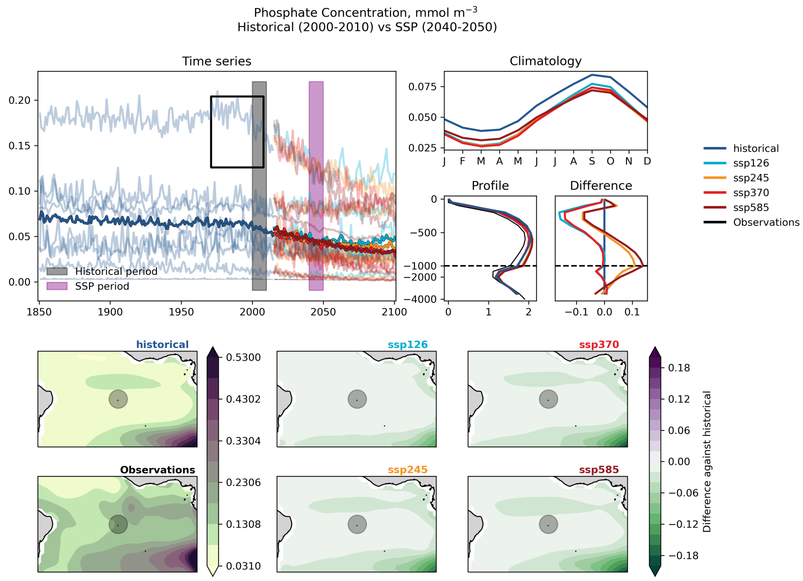
Phosphate Concentration, mmol m^{-3}
Historical (2000-2010) vs SSP (2040-2050)
Time series
Climatology
Profile
Difference
Historical period
SSP period
historical
ssp126
ssp245
ssp370
ssp585
Observations
Difference against historical

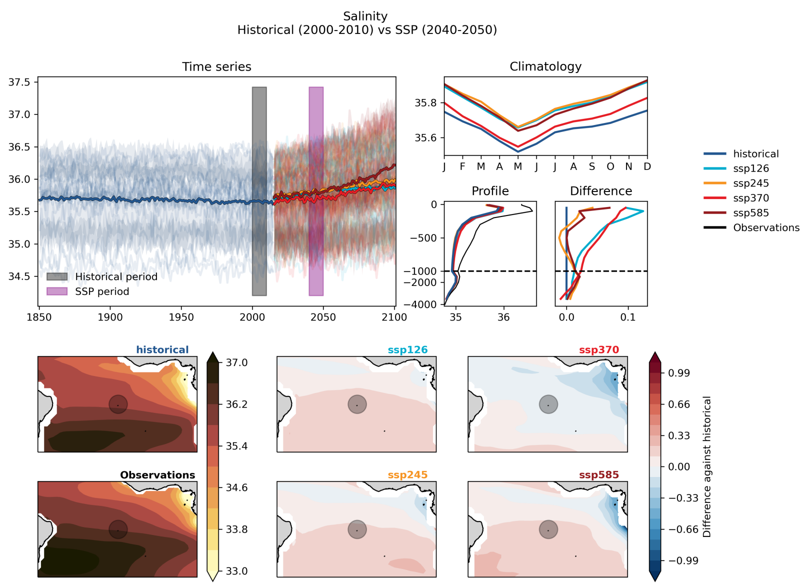
Salinity
Historical (2000-2010) vs SSP (2040-2050)
Time series
Climatology
Profile
Difference
Historical period
SSP period
historical
ssp126
ssp245
ssp370
ssp585
Observations
Difference against historical

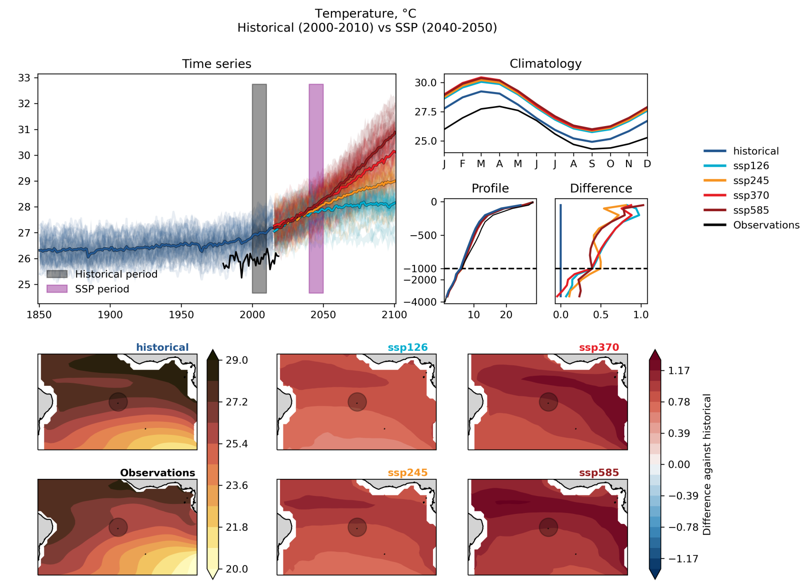
Temperature, °C
Historical (2000-2010) vs SSP (2040-2050)
Time series
Historical period
SSP period
Climatology
Profile
Difference
historical
ssp126
ssp245
ssp370
ssp585
Observations
Difference against historical

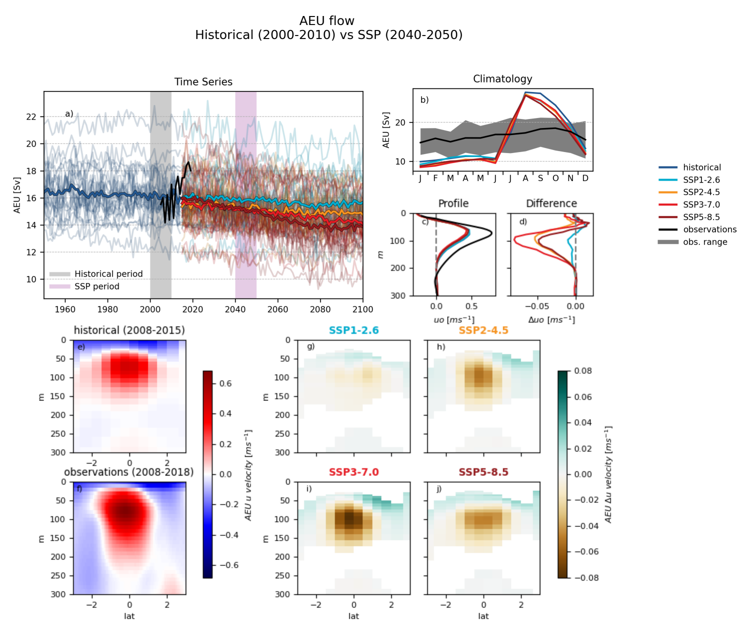
AEU flow
Historical (2000-2010) vs SSP (2040-2050)
Time Series
AEU [Sv]
Historical period
SSP period
Climatology
Profile
Difference
historical
SSP1-2.6
SSP2-4.5
SSP3-7.0
SSP5-8.5
observations
obs. range
historical (2008-2015)
observations (2008-2018)
AEU u velocity [ms⁻¹]
AEU Δu velocity [ms⁻¹]
lat


AI MPA
AEU transect
Study Area

Impacts of Climate Change on the Ascension Island Marine Protected Area and its ecosystem services

L. de Mora [1], G. Galli[1], Y. Artioli[1], S. Broszeit[1], D. Baum[2], S. Weber[3], J. Blackford[1]

[1]Plymouth Marine Laboratory, Prospect Place, The Hoe, Plymouth, Devon, UK, PL1 3DH
[2]Ascension Island Government, Ascension Island, South Atlantic Ocean, ASCN 1ZZ
[3]Centre for Ecology and Conservation, University of Exeter, Penryn Campus, Cornwall, UK TR10 9FE

Key Points:

- For the first time, a projection focused on the marine circulation and biogeochemistry of the Ascension Island MPA is presented.
- The MPA region will become warmer, more saline, more acidic, with less nutrients, less chlorophyll and less primary production.
- Even low emissions projections forecast significant changes within the MPA and these changes can impact ecosystem services.

Corresponding author: Lee de Mora, `ledm@pml.ac.uk`

Abstract

This is the first forecast of marine circulation and biogeochemistry for the Ascension Island Marine Protected Area (MPA). MPAs are a key management tools used to safeguard ocean biodiversity from human impacts, but their efficacy is increasingly threatened by anthropogenic climate change. To assess the vulnerability of individual MPAs to climate change and predict biological responses, it is first necessary to forecast how local marine environments will change. We found that the MPA will become warmer, more saline, more acidic, with less nutrients, less chlorophyll and less primary production by the mid-century. A weakening of the Atlantic equatorial undercurrent is forecast in all scenarios. In most cases, these changes are more extreme in the scenarios with higher greenhouse gases emissions and more significant climate change. The mean rise in temperature is between 0.9 °C and 1.2 °C over the first half of the 21st century. The integrated primary production and nutrients are forecast to decline in the MPA, but there is less consistency between models in projections of salinity, surface chlorophyll, and dissolved oxygen concentration at 500m depth. The combined effects of these projections may lead to changes in ecosystem services around Ascension Island. The effects of the model outputs were interpreted for three key ecosystem service providing habitats: biogenic deep sea habitats, intertidal sand and intertidal rocky shores. The outcomes were then used to assess potential effects on eight marine and coastal ecosystem services and information was compared to current ecosystem service levels.

Plain Language Summary

Ascension Island is a small remote volcanic island in the equatorial Atlantic Ocean. The seas around the Ascension Island have been protected from fishing and deep sea mining since 2019. We use the marine component of computer simulations of the Earth's climate to try to predict the future of the Ascension Island Marine Protected Area. Over the next century, the MPA region will become warmer, more saline, more acidic, with less nutrients, less chlorophyll and less primary production in the surface waters. The main current of the region, the Atlantic equatorial undercurrent, is also forecast to weaken in all scenarios. These changes will negatively impact the capacity of the area to provide ecosystem services such as the removal of carbon dioxide from the air, healthy ecosystems, as well as tourism and fish stocks. This work is important because it is the first assessment of the region since the protected areas creation in 2019, and will allow policy makers to understand how the changing climate is likely to affect their environment and ecosystem services.

1 Introduction

Unsustainable fisheries and anthropogenic climate change rank as the most pervasive drivers of marine biodiversity loss worldwide, threatening to undermine ocean health and human well-being alike (Jaureguiberry et al., 2022). Conservation efforts aimed at curbing these losses often centre around the establishment of marine protected areas (MPAs). Notably, there are ambitious global targets proposed to delivering 30% MPA coverage by 2030 (Woodley et al., 2019). This minimum protection fraction greatly exceeded the 2.18% of the ocean that was protected as recently as recently as the year 2016 (O'Leary et al., 2016).

Appropriately managed and enforced MPAs have proven to be highly effective in reducing and reversing fisheries impacts. Beyond their benefits to ecosystem health, MPAs have multiple socioeconomic benefits. Even small reserves can increase the abundances of local fishing stock (Hansen et al., 2011), and can also improve local social capital (Maina et al., 2011). Large scale remote marine wilderness MPAs can have fish biomass several times greater than recently fished MPAs with a significantly more diverse marine ecosystem community (Graham & McClanahan, 2013). However, even highly-protected MPAs remain vulnerable to extrinsic threats from climate change. Climate change has the potential to fundamentally degrade the ecosystems that MPAs are intended to protect (Bruno et al., 2018). Marine species follow shifting environmental niches, and their distributions are moving an order of magnitude faster than those on land (Bruno et al., 2018). This rapid change threatens to disrupt spatial overlap with existing MPA networks. Within MPAs, species and habitats are also exposed to many of the same climate change induced pressures that affect unprotected areas. These stresses include thermal stress, ocean acidification and altered trophic webs (du Pontavice et al., 2020). Given the potential of the changing climate to compromise MPA efficacy, many recent studies have stressed the need to incorporate 'climate smart' principles into MPA design and management and called for robust assessments of how local marine environments are likely to change in future (Tittensor et al., 2019; Wilson et al., 2020; O'Regan et al., 2021).

In the global context, the ocean's mean surface temperature is projected to increase by an average of 0.86 - 2.89 °C between 1995-2010 and 2081-2100 (Lee et al., 2021; Fox-Kemper et al., 2021). This rise will lead to cascading impacts on ocean physics and biogeochemistry. Empirical data indicates that the upper ocean has become more stably stratified since 1970 over the vast majority of the globe (Eyring et al., 2021). The enhanced stratification results in decreased nutrient availability in surface waters and associated reductions in primary production and faunal biomass (Lotze et al., 2019). There is high confidence that many ocean currents will change as a result of changing wind stress (Richter & Tokinaga, 2022; Weijer et al., 2020). Increased water temperatures, greater stratification, and weaker overturning circulation will result in reduced dissolved oxygen concentrations and expansion of biologically impoverished oxygen minimum zones (Stramma et al., 2012; Breitburg et al., 2018). In addition to temperatures, the uptake of anthropogenic CO_2 has also driven the acidification of the global ocean (Lee et al., 2021)

The cumulative impacts of these changes on marine biodiversity are already being observed in many protected and non-protected areas (Poloczanska et al., 2016; Bates et al., 2019). However, the effects of climate change are far from uniform. Projected changes in ocean temperature and biomass often exhibit latitudinal gradients as well as both fine-scale and basin-scale variation (Lotze et al., 2019). Ocean circulation patterns are also expected to have complex and variable responses to climate change, with some currents systems projected to intensify while others weaken (Richter & Tokinaga, 2022; Weijer et al., 2020). Robust local and regional forecasts are therefore necessary to predict likely biological responses and assess the vulnerability of individual MPAs (Tittensor et al., 2019). Unfortunately, such local forecasts are generally lacking, meaning that climate change is often framed in MPA management plans as a nebulous threat, without specific impact assessments or adaptation measures (O'Regan et al., 2021).

In this study, we develop the first climate forecast for the Ascension Island MPA (AIMPA) in the tropical South Atlantic, fig. 1. The AIMPA was designated in 2019 and covers the entirety of the 445,000 km^2 exclusive economic zone surrounding the UK overseas territory of Ascension Island, making the AIMPA one of the largest protected areas in the ocean. The MPA prohibits all forms of commercial fishing and mining, except small scale recreational and sports fishing are permitted in inshore waters. The MPA supports globally-important nesting populations of seabirds and green turtles (Weber et al., 2014; Weber & Weber, 2019), harbours a unique inshore fish and invertebrate assemblage (Wirtz et al., 2017), and encompasses large expanses of open ocean habitat that were previously exploited by longline vessels targeting tuna and swordfish. The AIMPA Management Plan lists climate change as one of the major remaining threats to biodiversity in the region (Government, 2021). However, little is known about the climate forecast for this specific region with which to predict ecological responses

Figure 1. Map showing the Ascension Island Marine Protected Area (AIMPA), the Atlantic Equatorial Undercurrent (AEU) transect and the study area.

We first assess how eight oceanographic bulk properties will evolve in the AIMPA over the 21^{st} century Using data from the coupled model inter-comparison project (CMIP6). The forecasts cover a range of representative emission scenarios and shared socio-economic pathways. We access these bulk properties in terms of their including seasonal, spatial and vertical patterns behaviour. We then examine how broad-scale ocean circulation patterns in the region will change, focusing specifically the Atlantic Equatorial Undercurrent (AEU) which has a pervasive influence on the oceanography of Ascension Island (Brandt et al., 2021). The AEU flows eastwards along the equator (3°S to 3°N) above 250 m depth and with its core at approximately 80 m. It then up-wells in the Gulf of Guinea, delivering nutrient rich, cooler subsurface water to the Southern Equatorial Current's cold tongue that flows eastward. This gives rise to a high productivity and low oxygen zone that protrudes westward south of the equator, where Ascension Island is located. Previous work has reported a weakening of the Atlantic cold tongue over recent decades (Tokinaga & Xie, 2011). However, to our knowledge there are few published projections of how the AEU will respond to climate change (Giarolla et al., 2015) and no recent analysis from CMIP6.

Finally, we assess how projected changes affect ecosystem survey provision in the Ascension MPA based on eight measures. We anticipate that the results of study will enable more robust predictions of biological responses to climate change in the AIMPA and in the wider tropical Atlantic region, helping to inform site-specific vulnerability assessments and adaptation plans.

Exploitation and climate change have been identified as the two most important drivers of marine biodiversity loss (Jaureguiberry et al., 2022, & references therein). This puts both marine ecosystems and human well-being at jeopardy because of the intrinsic link between biodiversity and the ecosystem services they provide (Watson & Zakri, 2005). Ecosystem services are the direct and indirect contributions of ecosystems to human well-being (Sukhdev et al., 2010) and are usually assessed in terms of the potential of an ecosystem to provide a service rather than if the service is used. This means that even though the AIMPA is a no-take region, it is still assessed in terms of potential ecosystem provision under climate change. deep sea ecosystem services are not well studied in general, but the Ascension Island marine ecosystem services in particular has been assessed recently (Wirtz et al., 2017; La Bianca et al., 2018; Barnes et al., 2019).

2 Methods

After a brief description of the CMIP6 framework, the analysis of this work is split into three parts. Most indicators were provided directly in CMIP6 and were analysed using a common framework. Secondly, the AEU required additional processing in a separate software tool. A third section describes the ecosystem service assessment methodology.

2.1 CMIP6

The data that were used to generate this analysis were global scale models from the sixth coupled model inter-comparison project (CMIP6) (Eyring et al., 2016). CMIP6 is an international collaborative project which allows modelling groups from around the world to share and compare their climate model output datasets. To participate, models are required to meet standards both in terms of scientific model quality, but also in terms of data formatting.

CMIP6 includes models with very small biases in the mean state and variability of the tropical Atlantic and The equatorial Atlantic warm sea surface temperature and westerly wind biases have been mostly eliminated in these models, relative to the previous inter-comparison (CMIP5) (Richter & Tokinaga, 2022). Furthermore, the seasonal and inter-annual variabilities of CMIP6 models in the equatorial and subtropical Atlantic compares favorable to the ERA-5 analysis, which suggests that they should be useful tools for understanding and predicting variability patterns for MPA (Richter & Tokinaga, 2022). Within CMIP6, each model typically includes multiple simulations of the recent past and the future. The historical simulations cover the years 1850-2015, and the future scenarios cover 2016-2100. Multiple future scenarios have been developed to cover several potential evolution of social and economic drivers resulting in different atmospheric concentration of greenhouse gases (O'Neill et al., 2016).

This work includes the scenarios: SSP1-2.6, SSP2-4.5, SSP3-7.0 and SSP5-8.5, described in (Riahi et al., 2017). These scenarios cover a wide range of possible futures, including sustainable development in the SSP1-2.6 scenario and the "middle of the road" pathway in SSP2-4.5, which extrapolates historic and current global development into the future with a medium radiative forcing by the end of the century. The regional rivalry scenario, SSP3-7.0, revives nationalism and regional conflicts, pushing global issues into the background which results in higher emissions. Then finally, the enhanced fossil fuel development in SSP5-8.5 is a forecast with the highest feasible fossil fuel deployment and atmospheric carbon concentration.

In practice, CMIP6 modelling groups produce simulations for multiple scenarios, and often produce more than one simulation per scenario. Each individual simulation of a scenario is called an ensemble member. Ensemble members for a given model usually have differences in their initial conditions, as the conditions of the climate at the start of the historical period are unknown but may have a significant influence of the evolution of the whole climate system. There is a wide variability in the number of ensemble members between models. For instance, the UKESM1 model produced 19 different variants for the historical experiment, each using slightly different initial conditions (Sellar et al., 2020). To fairly balance models with many simulations against models that only include one ensemble member, the "one model – one vote" weighting scheme is used. This means that each model is weighted equally in the multi-model mean. In practice, each ensemble member is weighted inverse proportional to the number of ensemble members that the model contributes. No effort was made here to bias the results in terms of model quality or historical performance.

2.2 Common framework analysis

The analysis was performed for the following variables in the MPA region: temperature, salinity, mixed layer depth, oxygen concentration at 500m, pH, nitrate, phosphate, chlorophyll and primary production. These are all variables that are directly produced in CMIP6 and can be analyses without any significant pre-processing. The multi-model ensemble analysis was generated using the method described here. Every model and ensemble member that satisfied the following conditions was included:

- Monthly Ocean data available on JASMIN over the full-time range (1850-2015 or 2015-2100).
- The cell area metadata ('areacello' file) was also available on JASMIN compute system, described below.
- The model data was compatible with ESMValTool, described below.
- Each contributed ensemble member must have both a historical and a future simulation.

Each variables analysis included the time evolution of the average value in the Ascension Island MPA area, the present and future average monthly climatology, the average and projected change in the depth profile, and the spatial distribution and projected change in the wider tropical Atlantic region. The time series are provided for the whole duration of the CMIP6 simulations (1850 to 2100). The others fields are provided for two 10 years periods: 2000-2010 to represent the current state and 2040-2050 to represent the mid-century climate.

Unless otherwise specified, surface model outputs are used in the analysis. The average time series, monthly climatology and vertical profile for the Ascension Island MPA are calculated using model outputs from a square region of 6 ° by 6°, centered on Ascension Island. As shown in fig. 1, the selected region is slightly larger than the real MPA. Given the typical model resolution, the small difference in area between the study region and the MPA is unlikely to affect the results. The "one model – one vote" scheme was used to calculate the multi-model weighted mean of the individual models. The model data was used "as is" with no effort to de-drift against pre-industrial control simulations.

Where possible, observational datasets from Obs4MIPS (Ferraro et al., 2015) were added for the region as a time series. In the case where time series data were not available for the MPA region, the observation data and time range were added as a transparent rectangle with black edges.

2.3 Atlantic equatorial undercurrent analysis

The properties of the AEU were analysed by focusing on the state and trend in the annual average flow, the changes in the monthly climatology, and the change in depth profiles. The mean annual AEU flow was estimated from each ensemble member by calculating the annual mean East-West zonal velocity values along a transect at longitude 23° West, between 3° South and 3° North and between the surface and 400m depth, as shown in fig. 1. This transect encompasses the whole AEU extension and coincides with the location of the Subsurface ADCP moorings, which are part of the PIRATA moor-

Table 1. The observational datasets used in this analysis and their references.

Field	Dataset	Reference
Temperature	WOA 2018	(Locarnini et al., 2018)
Salinity	WOA 2018	(Zweng et al., 2018)
MLD	IFerMER 2008	(de Boyer Montegut et al., 2004)
Oxygen	WOA 2018	(Garcia et al., 2018a)
pH	GLODAPv2 2016	(Olsen et al., 2016)
Nitrate	WOA 2018	(Garcia et al., 2018b)
Phosphate	WOA 2018	(Garcia et al., 2018b)
Chlorophyll	ESACCI-OC (2022)	(Sathyendranath et al., 2019)
Int. Primary Production	Eppley-VGPM-MODIS 2018	(Behrenfeld, 1997)
AEU	Tropical Atlantic Observing System	(Foltz et al., 2019; Brandt et al., 2021)

ing array (W. Johns et al., 2014; Bourlès et al., 2019; W. E. Johns et al., 2021), allowing for comparison with long-term moored observations (Foltz et al., 2019; Brandt et al., 2021).

The annual mean AEU flow values were obtained by taking the area-weighted sum of only the positive (West to East) velocity values in the transect area. To generate the monthly climatology, the monthly mean AEU flow values for present day (2000-2010) and future (2040-2050) periods were extracted from the dataset and averaged over each month. The depth velocity profiles for present day and future periods were derived from annual averaged velocity data as the average of the two grid cells closest to the equator, which represent the location of maximal velocity. As elsewhere, the "one model – one vote" weighting scheme was applied for the multi-model mean.

2.4 Ecosystem services assessment

Our assessment of climate change in CMIP6 was then used to assess the potential changes to marine ecosystem services provision around Ascension Island. We generated a literature review of current ecosystem services around Ascension Island. Then, the model data were then used to estimate changes to ecosystem services based on our literature review. A selection of supporting, regulating, provisioning and cultural ecosystem services relevant to the region were addressed. We targeted three key habitats in the assessment that were were chosen because their significance to the ecosystem services and their vulnerability in a changing climate. While it was beyond the scope of this work to carry out a full ecosystem services assessment, a recent ecosystem service assessment of the Ascension Island MPA was used to provide relevant information (La Bianca et al., 2018). The assessment of changes to ecosystem services was carried out in three steps:

- Identification of the key habitats contributing to each selected service were selected from a matrix of ecosystem services provided by each habitat (La Bianca et al., 2018).
- Using the model outputs, the habitats most sensitive to the changes modelled were selected, using the sensitivity analysis provided by (La Bianca et al., 2018).
- For each habitat selected in the first step, their contribution to the eight selected ecosystem services was taken from (La Bianca et al., 2018). Based on the sensitivity analysis, changes to each service were then forecast.

2.5 Hardware and software tools

The analyses were performed using the Earth System Model Evaluation Toolkit, ESMValTool (Righi et al., 2020). ESMValTool is a software toolkit that was built to facilitate the evaluation and inter-comparison of CMIP datasets. ESMValTool is built with a set of modular and flexible tools that allow it to quickly set up and develop analyses like this one. These tools include quick ways to standardize, slice, re-grid, and apply statistical operators to datasets. It is freely available, python-based, and built following standardised best coding practice: code review, documentation, unit testing, open discussions. ESMValTool is hosted on github and all the code used here is available (*ESMValTool: A community diagnostic and performance metrics tool for routine evaluation of Earth system models in CMIP github page*, n.d.). More details are below in the Code availability section.

Where available, observation-based data products were also included in the analysis, as listed in tab. 1. Existing Obs4MIPs data (Ferraro et al., 2015) were prioritised because of their availability and their compatibility with ESMValTool. Obs4MIP is a limited collection of observational datasets that has been pre-processed to resemble modelled CMIP datasets in terms of their formatting, grids, and interpolated to facilitate comparison against climate models.

This analysis was performed on the Centre for Environmental Data Analysis's (CEDA) JASMIN computing system (*Centre of Environmental Data Analysis, JASMIN compute machine*, n.d.). The size of the full CMIP6 data is so large that no data centre can host it in its entirety. This analysis was limited to the data locally available to JASMIN at the time the analysis ran (January 2022). Furthermore, some models were excluded because their outputs did not strictly adhere to the CMIP6 standard formats, making them fundamentally incompatible with our software analysis framework.

3 Results

A summary of the analyses are shown in fig. 2. This figure summarises the predicted direction of travel of the CMIP6 ensemble for each field. In this figure, each pane represents a different field, and the colours represent the different forecast scenarios. For each scenario, a horizontal bar shows the multi-model mean of the anomalies between the mid-century forecast and the recent past. The vertical line of each scenario represents one standard deviation either side of the mean, and is absent in the cases where there are only one contributing model. In all cases, the data shown here is the mean of the anomalies, not the anomaly of the means.

The results of each individual analysis are shown first and then the AEU analysis. For all fields, the multi-model mean for the period 2000-2010 and 2040-2050 and the standard deviation of the ensemble of single model-means is shown in tab. 2. The standard deviation is calculated as a measure of the spread of the single model means but does not include variability in the time dimension. Table 3 shows the number of models and total number of CMIP6 ensemble member for each field for each scenario.

3.1 Temperature

Figure 3 shows the summary results of the analysis for Ascension Island MPA sea surface temperature. While the models tend to overestimate the recent historical observational data, there is a clear warming signal in the region in all scenarios. The surface warms similarly in all scenarios by the year 2040, but there is a more significant divergence between the four future scenarios by the end of the analysis period in 2050. This divergence becomes even more significant towards the end of the century. The climatology pane shows that the models anticipate the observed seasonal cycle by approximately

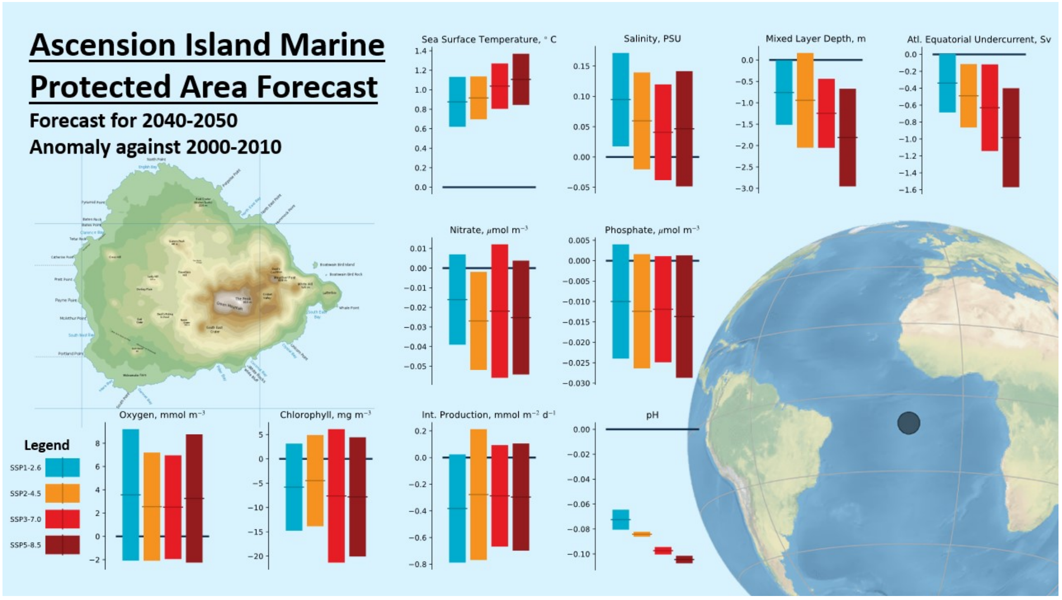

Figure 2. Summary of predicted climate change impacts on the biophysical oceanography of the Ascension Island MPA, based on CMIP6 ensemble projections. In these figures, the colour represents the different shared socio-economic pathway scenario, where light blue is SSP1-2.6, orange is SSP2-4.5, red is SSP3-7.0 and brown is SSP5-8.5. The y-axis shows the anomaly between the mid century forecast and the recent past (2000-2010). The mean of the multi-model mean is shown as a thin horizontal line and the wide lines represents the standard deviation. Note that, the anomaly is calculated first for each individual ensemble member.

Table 2. The multi-model mean the standard deviation of the ensemble of single model-means for each variable in the study. These values are calculated from the mean and standard deviation of the individual model ensemble means for the periods 2000-2010 in the historical period and 2040-2050 in the future scenarios. Fields with only a single model contributing do not include a value for the standard deviation. The surface value is shown, except for MLD, Oxygen, integrated primary production and the AEU.

Field	Units	Historical 2000-2010	SSP1-2.6 2040-2050	SSP2-4.5 2040-2050	SSP3-7.0 2040-2050	SSP5-8.5 2040-2050
SST	° C	27.0 ± 0.5	27.8 ± 0.4	27.9 ± 0.4	28.1 ± 0.4	28.1 ± 0.4
Salinity	PSU	35.7 ± 0.5	35.8 ± 0.5	35.8 ± 0.4	35.7 ± 0.5	35.8 ± 0.4
MLD	m	33.2 ± 8.2	33.9 ± 8.5	32.1 ± 8.1	33.0 ± 9.3	32.9 ± 8.7
Oxygen	mmol m^{-3}	69 ± 32	77 ± 27	76 ± 28	76 ± 29	76 ± 28
pH		8.05 ± 0.01	7.97 ± 0.02	7.96 ± 0.01	7.95 ± 0.01	7.94 ± 0.01
Nitrate	mmol m^{-3}	0.19 ± 0.24	0.20 ± 0.22	0.19 ± 0.23	0.19 ± 0.23	0.17 ± 0.22
Phosphate	μmol m^{-3}	0.058 ± 0.049	0.045 ± 0.040	0.043 ± 0.041	0.044 ± 0.041	0.044 ± 0.037
Chlorophyll	mg m^{-3}	121 ± 62	111 ± 63	112 ± 65	109 ± 61	113 ± 60
Int. PP	mmol m^{-2} d^{-1}	12.4 ± 3.7	11.2 ± 4.0	11.1 ± 4.0	11.2 ± 4.0	11.0 ± 3.8
AEU	Sv	16.2 ± 2.0	15.8 ± 2.0	15.2 ± 1.6	14.9 ± 1.6	14.7 ± 2.0

Table 3. The number of contributing models and the total number of contributing ensemble members. The total number of contributing ensemble members is shown in parentheses.

Field	Historical	SSP1-2.6	SSP2-4.5	SSP3-7.0	SSP5-8.5
SST	28 (123)	25 (110)	24 (68)	22 (116)	25 (77)
Salinity	26 (111)	22 (68)	23 (68)	20 (73)	22 (60)
MLD	20 (97)	9 (50)	19 (72)	7 (58)	8 (45)
Oxygen	9 (70)	8 (52)	8 (42)	8 (68)	8 (39)
pH	9 (36)	8 (32)	7 (22)	8 (47)	7 (22)
Nitrate	9 (19)	8 (19)	8 (12)	8 (19)	9 (13)
Phosphate	8 (18)	7 (18)	7 (11)	7 (18)	8 (12)
Chlorophyll	8 (57)	7 (41)	7 (35)	7 (48)	8 (35)
Int. PP	11 (26)	8 (28)	8 (29)	8 (27)	8 (12)
AEU	24 (77)	19 (61)	21 (55)	19 (66)	21 (60)

one month. The profile pane and profile difference panes show that the warming occurs throughout the water column, not just the surface layers. However, warming is more intense in the surface and subsurface layers than at greater depths. The surface map panes show that while the temperature increase is greatest near the equator in all future scenarios, the sea surface temperature rises everywhere in the region.

3.2 Salinity

Figure 4 shows the CMIP6 ensemble analysis for salinity in the Ascension Island MPA region. This figure shows that the model ensemble captures observational surface salinity in the region, but many models underestimate historical behaviour, as does the multi-model mean. In the future period, the annual mean salinity rises in all scenarios. In the years 2040-2050, the change in salinity is similar in all future scenarios. There are more significant differences in salinity between scenarios by the end of the century. Note that there is a discontinuity in the ensemble mean between the historical and the future scenarios at the year 2015. This is because the historical and future scenarios contain a slightly different set of models, as shown in tab. 3. The annual cycle of surface salinity in the MPA remains intact, but SSP5-8.5 shows a more significant rise in salinity. In the depth profile, the SSP5-8.5 and SSP2-4.5 scenarios seem to more closely follow the historical behaviour than SSP1-2.6 or SSP3-7.0. In the wider region, the distribution of sea surface salinity is strongly influenced by coastal effects off the Western African Coast, but all models show a rise in salinity in the equatorial regions and desalification in the Southern Atlantic, relative to the historical period.

3.3 Mixed Layer Depth

Figure 5 shows the CMIP6 ensemble analysis for the mixed layer depth. The model data here uses the "mlotst" CMIP6 field, which is the mixed layer depth calculated instantaneously on the model time step and uses a density criteria of 0.125 kg m^{-3} according to the CMIP6 protocol for the instantaneous model fields (Griffies et al., 2016). However, the observational data used are from (de Boyer Montegut et al., 2004) where MLD was calculated from water density with a fixed threshold criterion of 0.03 kg m^{-3}. This means that the observations and model ensemble are not strictly compatible here and should only be used to estimate differences in patterns. The model ensemble mean is comparable to observations but does not capture minimum MLD observed. In the climatological pane, a small shallowing of MLD is observed between June and November in all

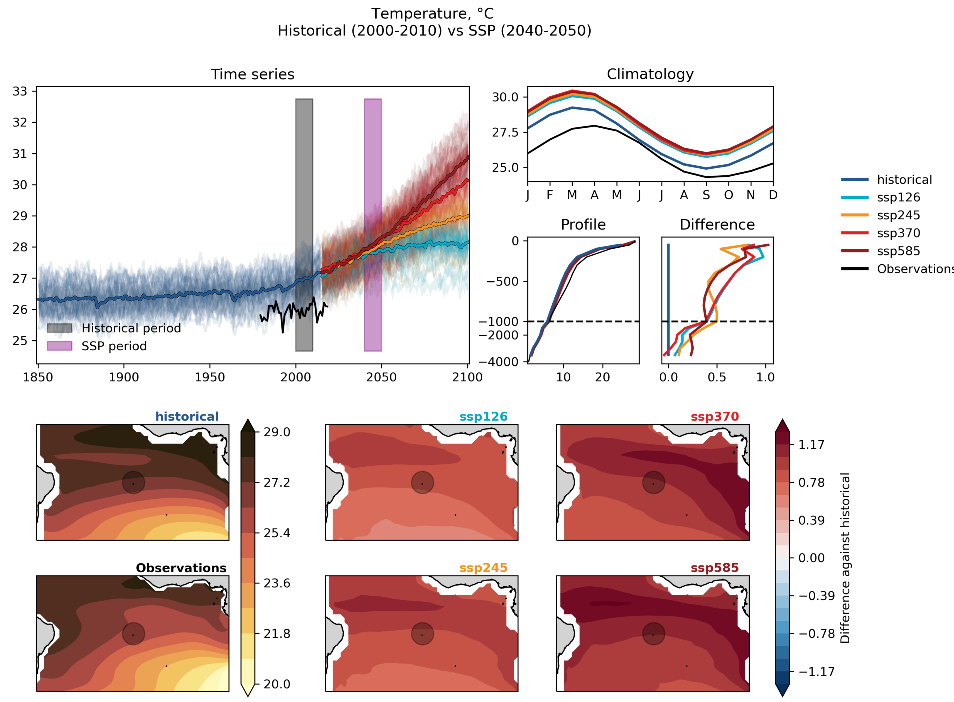

Figure 3. The CMIP6 ensemble temperature analysis for the Ascension Island MPA. The top left pane shows the MPA sea surface temperature in the historical period (blue) and multiple future scenarios (green, yellow, orange, red). Each model's range between the smallest and largest ensemble member at each point in time is shown separately as an overlapping semi-transparent coloured band. The observational data is shown as a black line. The black and pink vertical bars indicate the times where the historical and future periods are extracted in the other panes. The top right pane shows the monthly climatology. The profile and difference panes show the depth profiles and the difference against the historical depth profile. The lower six panes show the historical period, the observational dataset, and the difference between the four future scenarios and the historical model ensemble mean.

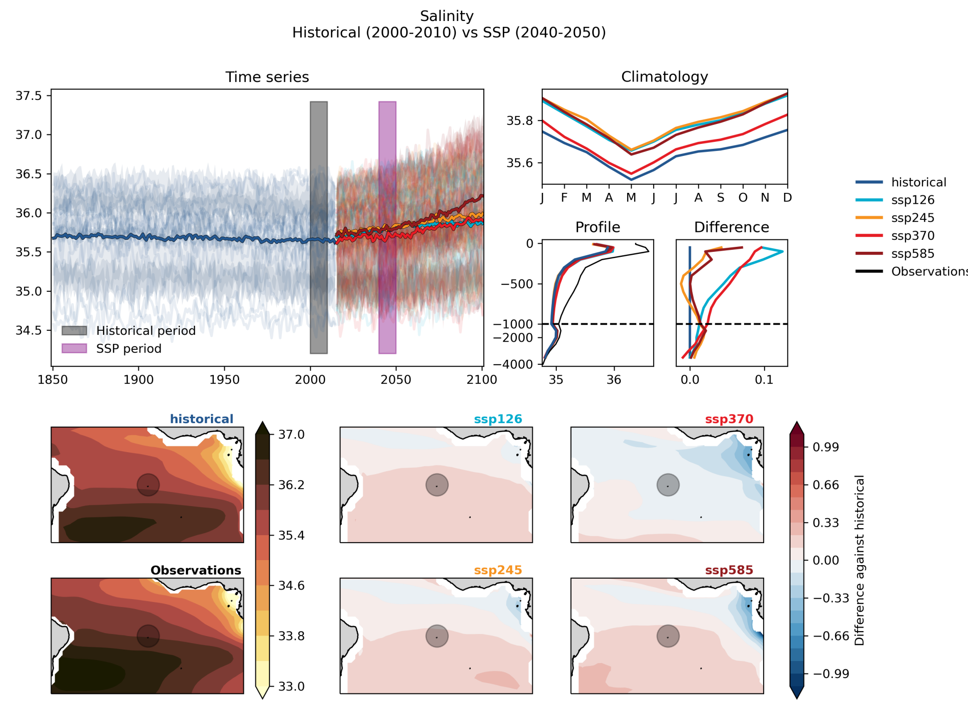

Figure 4. The CMIP6 ensemble salinity analysis for the Ascension Island MPA The top left pane shows the salinity in the historical period (blue) and multiple future scenarios (green, yellow, orange, red). Each model's range between the smallest and largest ensemble member at each point in time is shown separately as an overlapping semi-transparent coloured band. The observational data range is shown as a black box. The black and pink vertical bars indicate the times where the historical and future periods are extracted. The top right pane shows the monthly climatology. The profile and difference panes show the depth profiles and the difference against the historical depth profile. The lower six panes show the historical period, the observational dataset, and the difference between the four future scenarios and the historical model ensemble mean.

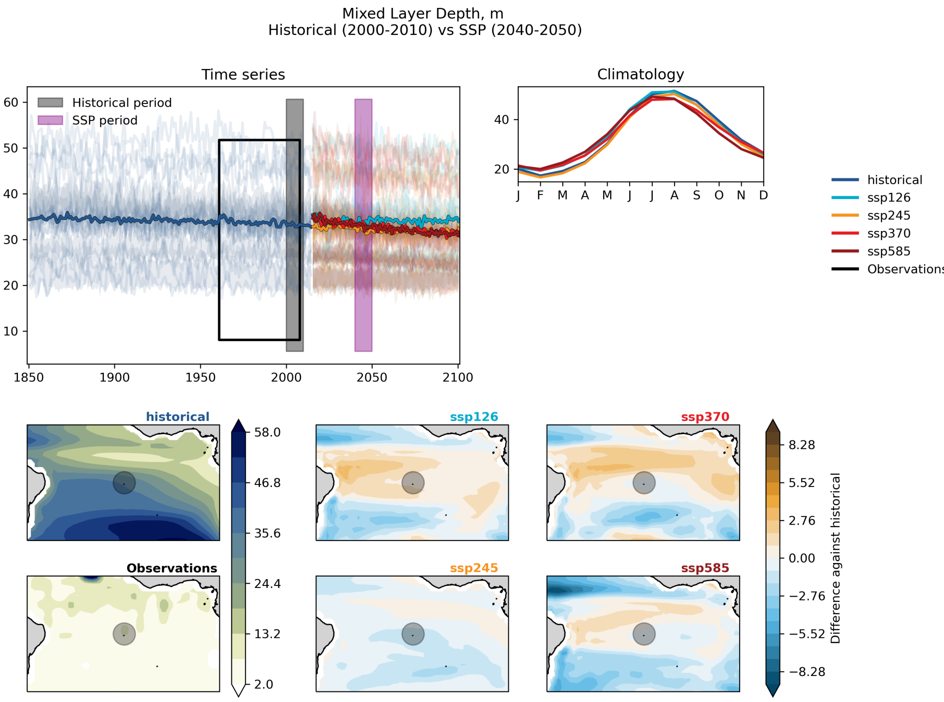

Figure 5. The CMIP6 ensemble mixed layer depth analysis. The top left pane shows the mixed layer depth in the historical period (blue) and multiple future scenarios (green, yellow, orange, red). Each model's range between the smallest and largest ensemble member at each point in time is shown separately as an overlapping semi-transparent coloured band. The observational data range is shown as a black box. The black and pink vertical bars indicate the times where the historical and future periods are extracted. The top right pane shows the monthly climatology. The lower six panes show the historical period, the observational dataset, and the difference between the four future scenarios and the historical model ensemble mean.

future scenarios relative to the historical period. As this is a 2D dataset, there are no depth profile panes. In the spatial distribution panes, only slight differences between scenarios can be seen in the MPA region, though the impact in the wider region is more significant, especially away from the equator. Unfortunately, the interpretation of the observational mixed layer depth is not straightforward – nevertheless, it is included for completeness.

3.4 Oxygen Concentration at 500m

The oxygen concentration at 500m is shown in fig. 6. The 500 m depth was selected because the observational water column minimum oxygen concentration occurs at 500m in the World Ocean Atlas data (Garcia et al., 2018a). In the time series, there is little agreement between models in either the historical or future times series. Indeed, there appears to be two diverging categories of behaviours. Some models project a strong decline and others an increase. The two behaviours cancel each other out in the ensemble mean resulting in a small change in oxygen at 500m in the MPA. However, this small change is an unlikely outcome, as very few models project it. This inter-model uncertainty is a result of oxygen concentrations being strongly influenced by simultaneous physical changes in solubility, circulation, and mixing and changes in biological sources and sinks (Kwiatkowski et al., 2020).

The oxygen at depth is particularly sensitive to how the hydrodynamics of the area represented, particularly stratification and circulation. High oxygen concentration is an indication of waters that have been recently in contact with the atmosphere (usually called "young") and lower oxygen indicates that waters have been trapped below surface for a longer period (usually called "old"). This may explain the strong difference in the historical period: models with higher concentrations of oxygen are likely to simulate current structures that includes younger waters at 500m depth, and the opposite for those with low oxygen concentration.

In addition, it can be seen in the spatial distribution pane of fig. 6 that the MPA sits between a region to the South where the oxygen concentration at 500m decreases and another region where it rises in the North. This means that the overall model mean is particularly sensitive to the placement of these two regions in the multi-model mean, the intensity of change in the two regions, but also the distribution of changes in the contributing individual models.

3.5 pH

Figure 7 shows the multi-model CMIP6 pH analysis for the MPA region. In the surface pH time series, there is a very tight agreement between models, but also between the models and the observations. Similarly, there is a very tight grouping for model forecasts. This is expected as the surface pH in open ocean waters is strongly linked to the atmospheric carbon dioxide concentration, and the atmospheric carbon concentration is a prescribed variable for the different emission scenario and is the same between all models. There is more divergence in the depth profile, as this is less strongly linked to the atmospheric forcing and is more influenced by marine circulation in a similar way to oxygen at 500m shown in fig. 6. The pH in the MPA is projected to decrease until the end of the century in all scenarios, with some models projecting some recovery at the end of the century in the low emission scenario, SSP1-2.6. It is important to note that even by mid-century the whole annual cycle of pH will be lower than the current minimum.

3.6 Nitrate and Phosphate

Figures 8 and 9 show the CMIP6 ensemble nitrate and phosphate analysis, respectively. While there is a significant diversity in the mean surface nutrients in the historical period, a small decline in annual mean surface nitrate can be seen in all models individually, and a more pronounced decline can seen in the surface phosphate in figure 9. The mean of the ensemble of models is relatively successful at reproducing the historical WOA nitrate values for the recent past. However, most of the models underestimate the observed phosphate values for the historical period. In the multi-model mean climatological averages for nitrate, there is a decline in the peak nutrients in July and November while the rest of the year has little change. In contrast, the multi-model mean climatological phosphate average forecasts an even year-round decrease under all scenarios. Changes in nutrient profile over the depth are generally, order 10% compared to typical historical values. There is a decline in nutrients for waters shallower than 500m, and an increase for deeper waters. This decline is likely due to increased stratification and reduced mixing, as seen in fig. 5. Due to the open ocean – low nutrients nature of the MPA, the absolute change in surface nitrate and phosphate concentration shown in the surface map is smaller than other regions of the South Atlantic. However the change predicted by the models in the MPA is about 50% in relative terms.

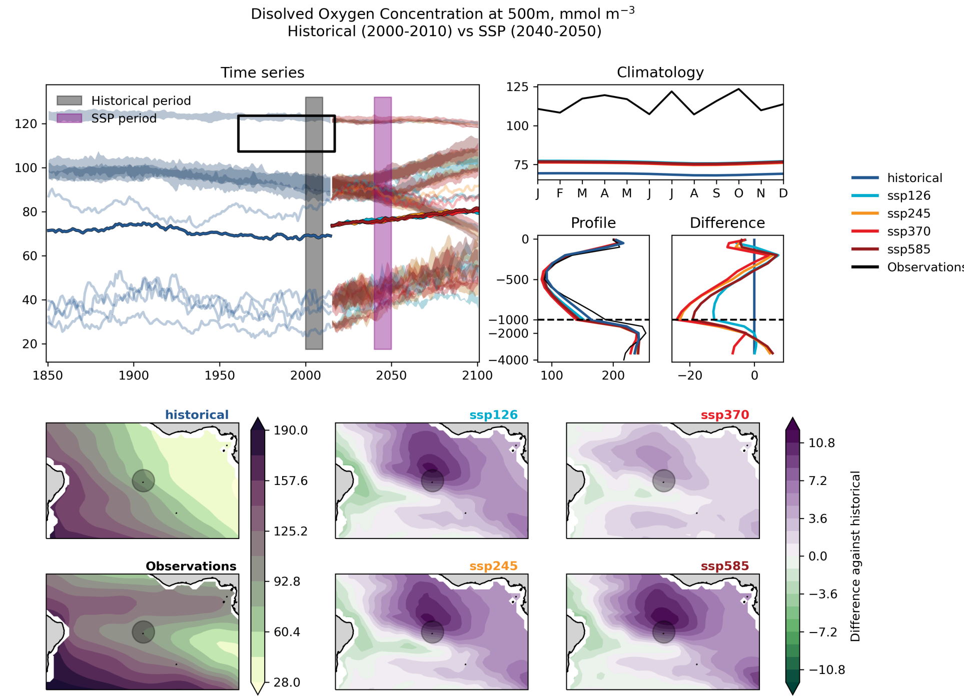

Figure 6. The Oxygen concentration at 500m depth in the CMIP6 multi model ensemble. The top left pane shows the dissolved oxygen concentration at 500m in the historical period (blue) and multiple future scenarios (green, yellow, orange, red). Each model's range between the smallest and largest ensemble member at each point in time is shown separately as an overlapping semi-transparent coloured band. The observational data range is shown as a black box. The black and pink vertical bars indicate the times where the historical and future periods are extracted. The top right pane shows the monthly climatology. The profile and difference panes show the depth profiles and the difference against the historical depth profile. The lower six panes show the historical period, the observational dataset, and the difference between the four future scenarios and the historical model ensemble mean.

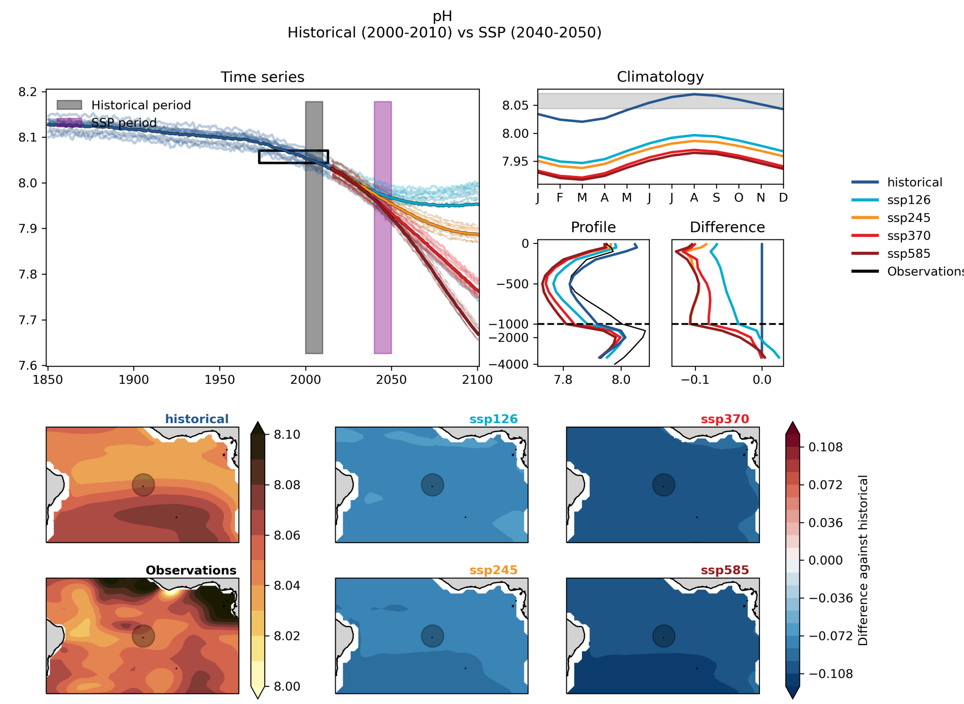

Figure 7. The surface pH in the CMIP6 multi model ensemble. The top left pane shows the annual mean surface pH in the historical period (blue) and multiple future scenarios (green, yellow, orange, red). The range between the smallest and largest ensemble member at each point in time is shown separately as an overlapping semi-transparent coloured band. The observational data range is shown as a black box. The black and pink vertical bars indicate the times where the historical and future periods are extracted. The top right pane shows the monthly climatology. The profile and difference panes show the depth profiles and the difference against the historical depth profile. The lower six panes show the historical period, the observational dataset, and the difference between the four future scenarios and the historical model ensemble mean.

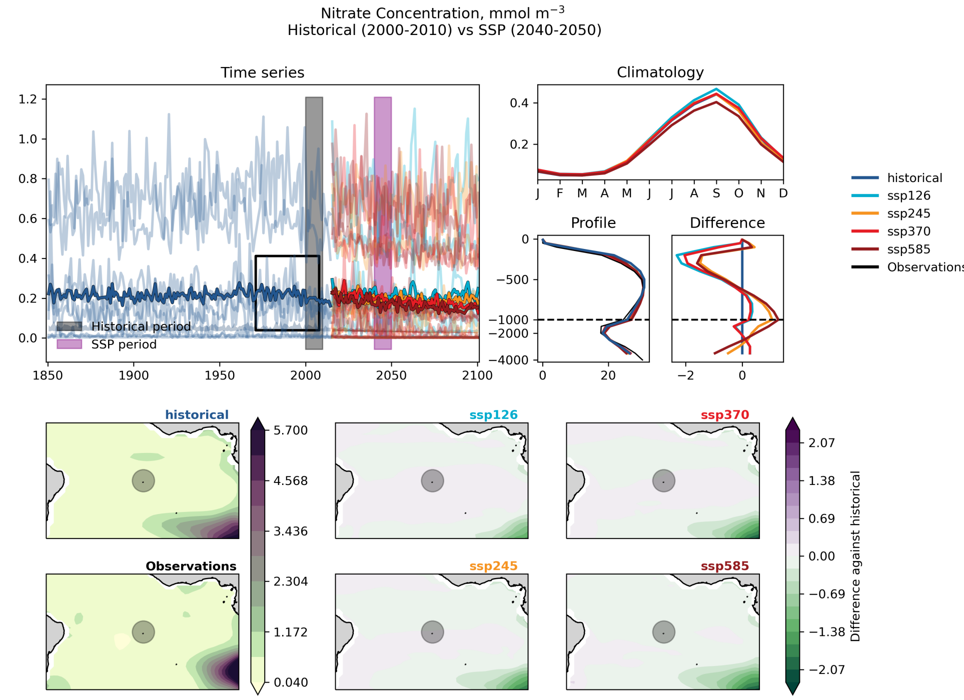

Figure 8. The surface nitrate concentration in the CMIP6 multi model ensemble. The top left pane shows the annual mean surface nitrate in the historical period (blue) and multiple future scenarios (green, yellow, orange, red). The range between the smallest and largest ensemble member at each point in time is shown separately as an overlapping semi-transparent coloured band. The observational data range is shown as a black box. The black and pink vertical bars indicate the times where the historical and future periods are extracted. The top right pane shows the monthly climatology. The profile and difference panes show the depth profiles and the difference against the historical depth profile. The lower six panes show the historical period, the observational dataset, and the difference between the four future scenarios and the historical model ensemble mean.

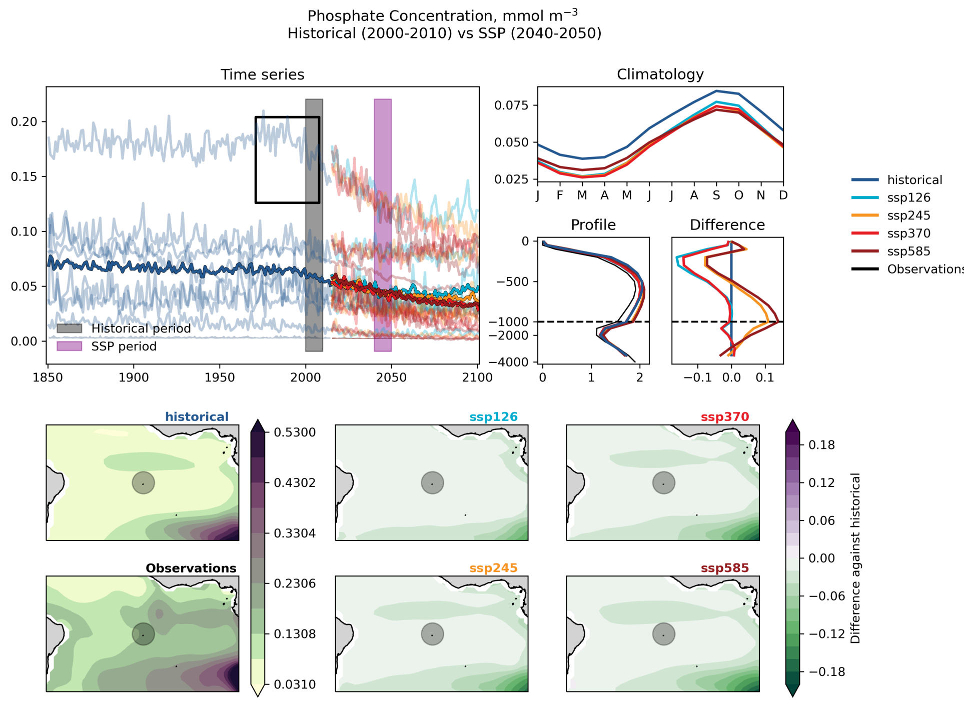

Figure 9. The surface phosphate concentration in the CMIP6 multi model ensemble. The top left pane shows the annual mean surface phosphate in the historical period (blue) and multiple future scenarios (green, yellow, orange, red). The range between the smallest and largest ensemble member at each point in time is shown separately as an overlapping semi-transparent coloured band. The observational data range is shown as a black box. The black and pink vertical bars indicate the times where the historical and future periods are extracted. The top right pane shows the monthly climatology. The profile and difference panes show the depth profiles and the difference against the historical depth profile. The lower six panes show the historical period, the observational dataset, and the difference between the four future scenarios and the historical model ensemble mean.

3.7 Chlorophyll

Figure 10 shows the CMIP6 ensemble mean chlorophyll analysis. Some models forecast a decline and others a rise in future surface chlorophyll in the MPA. The multi-model mean does reproduce the observational range for the region, but there is a significant diversity in the biases of individual models. In the future, the multi-model ensemble mean shows a decline in all scenarios in the mid-century. However, some models forecast a large rise in chlorophyll, but most show a small decline. For individual models, the change in chlorophyll is linked to the strength of the anthropogenic forcing of the scenario, but this does not hold for the multi-model mean.

While ensembles climatological mean show a seasonal cycle in the surface chlorophyll, it does not fully capture the present seasonal cycle seen in the observations: the annual peak is delayed by one month, and is significantly less extreme. The ensemble mean also has an extended annual minimum while the annual minimum in the observations is much more brief and earlier in the year. In the future forecast, the models project that the shape of the seasonal cycle of surface chlorophyll will remain, but the peak will be reduced, indicating a less active bloom. In the spatial distributions, the ensemble mean reproduces much of the wider patterns in historical observations in the Southern Atlantic, especially the higher production of the equatorial Atlantic, and the lower production in the Southern gyre.

3.8 Integrated primary production

Figure 11 shows the CMIP6 ensemble integrated primary production analysis. The multi-model mean does closely match the observational mean over the recent historical past, but fails to capture the inter-annual variability in the observational data. Several of the single models show variability of similar order to the observational data. Both the single models and the multi-model mean have very little trend over the historical period, but both do show some changes in the forecast period. Like the chlorophyll in fig. 10, most models forecast a decline but some models show a rise in integrated primary production. When combined, the declining models overwhelm the rising models and the multi-model mean forecast declines relative to the historical period. Like the chlorophyll data, the ensembles climatological mean show a seasonal cycle in the surface chlorophyll, but it does not fully capture the present seasonal cycle seen in the observations: the annual peak is delayed by one month, and is less extreme. The model bloom also extends later in the year than in the observational record. In the forecasts, the climatological behaviour retains the same shape, but shows a even negative bias across the whole year. In the wider region, all scenarios show a decrease in the multi-model mean integrated primary production over the equatorial Atlantic region, with the largest changes closer to the equator in SSP3-7.0 and SSP5-8.5. The primary production is influenced by nutrient availability, which is linked to the mixed layer depth, as well as linked to temperature and light.

3.9 Atlantic Equatorial Undercurrent Analysis

The analysis of the Atlantic Equatorial Undercurrent is shown in fig. 12. Pane a of fig. 12 shows the time evolution of the mean annual AEU flow in the historical and future scenarios, compared with observational estimates for the 2005-2019 period (Brandt et al., 2021). The average value of the AEU flow during the historical period is 16.3 Sv and ranges between 12.8 Sv and 21.5 Sv. This is well within the range of values reported in the literature, between 14.0 Sv and 18.0 Sv (Hormann & Brandt, 2007; Brandt et al., 2021). Little change is detected in the AEU flow during the historical period, but all future scenarios display a decrease in mean annual flow. The decrease is minimal in the more moderate climate change scenarios, for instance -0.07 Sv/decade in SSP1-2.6 and -0.3 Sv/decade in SSP5-8.5. In the high emission scenario, SSP5-8.5, the AEU decreases

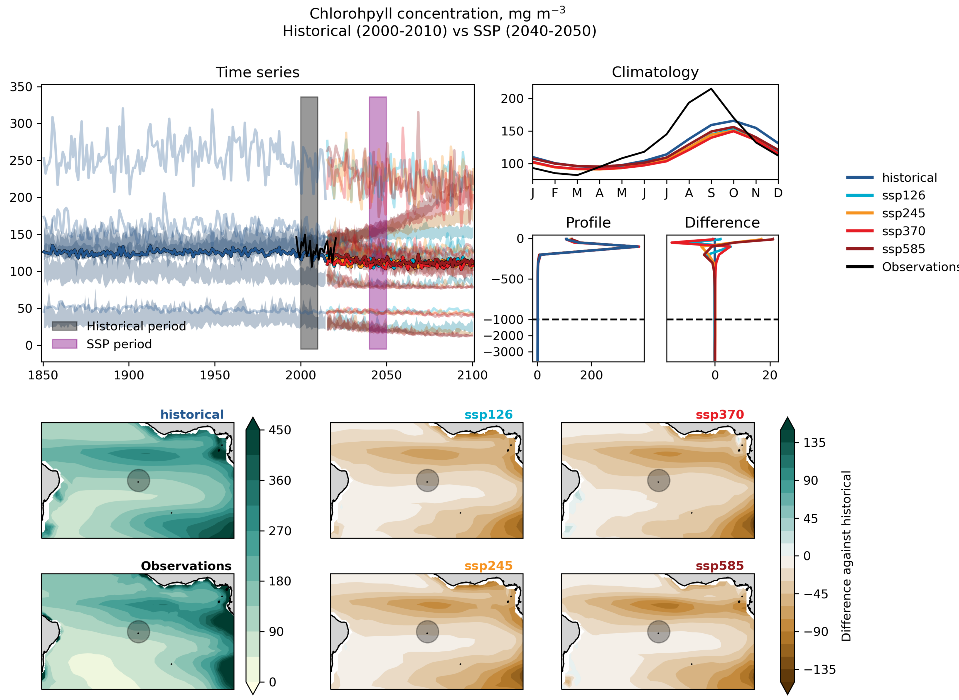

Figure 10. The surface chlorophyll concentration in the CMIP6 multi model ensemble. The top left pane shows the annual mean surface chlorophyll concentration in the historical period (blue) and multiple future scenarios (green, yellow, orange, red). The range between the smallest and largest ensemble member at each point in time is shown separately as an overlapping semi-transparent coloured band. The observational data time series is shown as a black line. The black and pink vertical bars indicate the times where the historical and future periods are extracted. The top right pane shows the monthly climatology. The profile and difference panes show the depth profiles and the difference against the historical depth profile. The lower six panes show the historical period, the observational dataset, and the difference between the four future scenarios and the historical model ensemble mean.

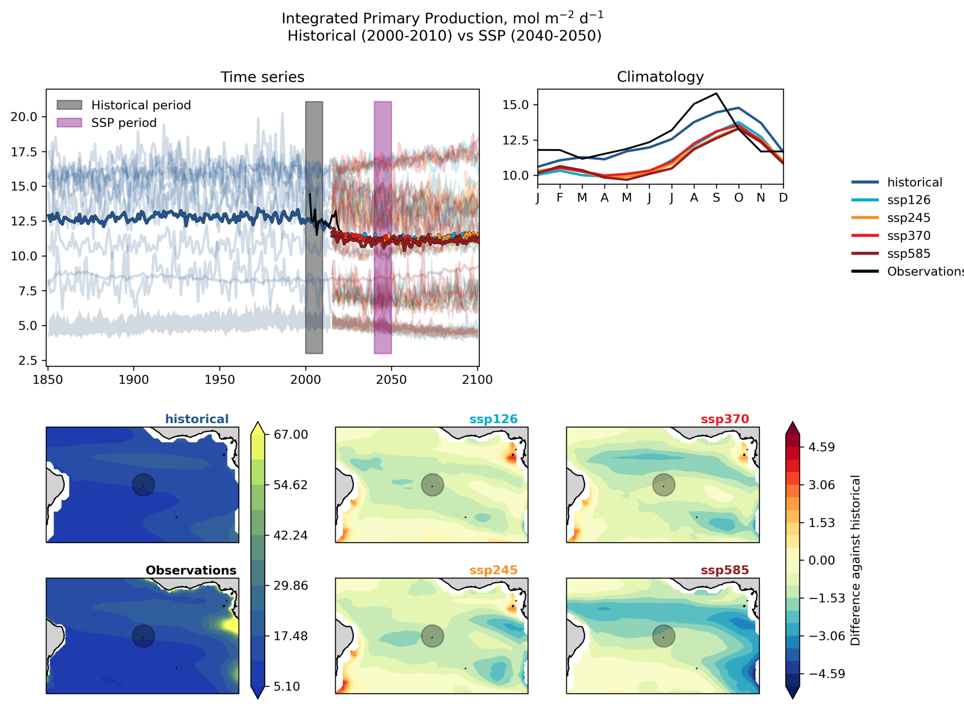

Figure 11. The Integrated Primary Production in the CMIP6 multi model ensemble. The top left pane shows the annual mean depth-integrated primary production in the historical period (blue) and multiple future scenarios (green, yellow, orange, red). The range between the smallest and largest ensemble member at each point in time is shown separately as an overlapping semi-transparent coloured band. The observational data time series is shown as a black line. The black and pink vertical bars indicate the times where the historical and future periods are extracted. The top right pane shows the monthly climatology. The lower six panes show the historical period, the observational dataset, and the difference between the four future scenarios and the historical model ensemble mean.

Table 4. Change in the AEU in mid-century and end of century forecasts.

SSP SSP	% Change 2040-2050 vs 2000-2010	% Change 2090-2100 vs 2000-2010	Trend Sv/decade
historical	-	-	-0.07
SSP1-2.6	-1.8	-3.2	-0.07
SSP2-4.5	-5.3	-7.6	-0.10
SSP3-7.0	-6.4	-11.5	-0.15
SSP5-8.5	-6.1	-14.2	-0.30

by 6.1% by 2050 and by 14.2% by 2100. The rate of change is relatively constant throughout the scenario period, except for in the SSP5-8.5 scenarios, where the bulk of change happens during the second half of the century.

The work of (Brandt et al., 2021) looked at long-term mooring observations and detected a strengthening of the AEU by 20% in the 2005-2019 period. They attributed it to multi-decadal climate variability that characterizes the equatorial Atlantic. This means that while a trend is observed over the observational period, the authors did not think it was likely to be caused by human activity, but rather it is part of the natural variability of the undercurrent. Whereas there's no trace of such an upwards trend in the historical simulation, such a variation over a relatively short time span, compared to the centennial timescale here represented, lies within the range of the multi-model ensemble. Also it is worth remembering that ESM simulations are not meant to correctly represent the phase of the climate system nor the exact timing of climate variability. In fact, as the authors of the study pointed out, the detected change is to be attributed to multi-decadal variability rather than to long term (climate change related) trends.

The annual cycle of the CMIP6 AEU (2000-2010) is shown in fig. 12b , along with the range of values reported by (Brandt et al., 2021). The multi-model mean shows a clear seasonal behaviour with lower transport in January-June and higher transport during July-December. While observations show a similar timing of the seasonal maximum and minimum, the amplitude of the seasonal cycle is much higher in the models than in the observations. There is a clear two-phase pattern (low transport from January to June, peak and decline from July to December), which is absent from the observations. The models have a peak current more than double of the winter minimum while the average peak is about 20% higher than the minimum winter value in the observations.

The depth velocity profile at the equator is shown in pane c of fig. 12. The model velocity profile agrees with observations in placing the bulk of the AEU between 50m and 200m depth (Brandt et al., 2021), with models simulating a smaller peak velocity and a narrower current. A weakening of the AEU is observed in the future scenarios, taking place mostly at and below the AEU core.

Panes e and f of fig. 12 show the comparison between the CMIP6 average profile and the AEU velocity profile along the AEU transect reconstructed from (Brandt et al., 2021)at 23°West. Overall, the main features of the AEU are well captured by the model average despite the CMIP6 ensemble average appears to overestimate the latitudinal extension of the current (together with smaller peak and depth extension shown also in fig. 12 pane c. This is to be expected given the coarse resolution of the CMIP6 models and the fact that averaging over many members has the effect of smoothing out peak values.

The remaining panes of fig. 12, panes g, h, i and j show the difference between the mean AEU velocity field in the four future scenarios for the years 2040-2050 and the historical ensemble in the years 2000-2010. Negative currents flowing from East to West

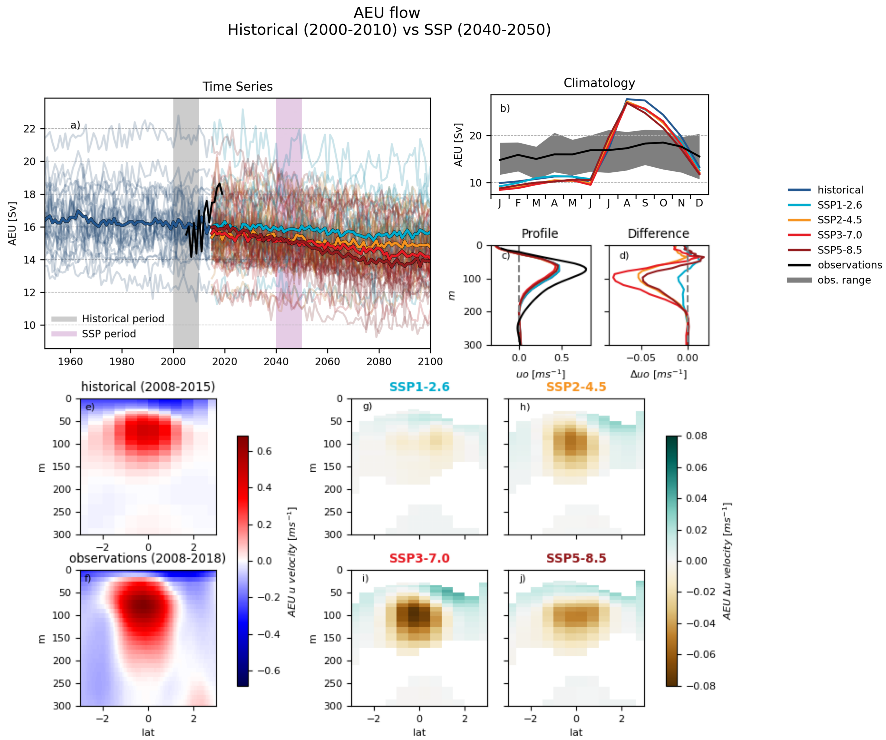

Figure 12. a) Atlantic Equatorial Undercurrent mean annual flow time series compared with flow estimated from observations (2005-2019). Solid lines are historical and scenario averages, shaded lines are individual models. b) Monthly mean AEU flow climatology for historical period and four scenarios (solid lines), the grey area represents the range of estimates from observations. c) monthly mean velocity depth profile at the equator for historical and four scenarios, compared with observational data (2008-2018), and d) difference between scenario and historical data. e) ensemble averaged AEU velocity at 23°W (2008-2015) and f) velocity field reconstructed from observations (2008-2018). g), h), i), j) velocity field difference between the four scenarios and the historical runs, maps show only eastbound velocity differences. All observational data from (Brandt et al., 2021)

were masked to highlight changes in the AEU alone. All scenarios show a weakening of the velocity field between 75m and 200m depth. This is partially counterbalanced by an increase in velocity at shallower depths. The future scenario that shows the maximum local change is SSP3-7.0, where the peak velocity decreases by around 0.08 m s^{-1}. This reduction in peak velocity is partly balanced by an increase in velocity in the shallower and northward region so that the annual mean current in this scenario by 2050 is close to that projected in the higher emission scenario (fig. 12, pane a). After 2050, the two scenarios diverge with the strongest weakening of AEU being projected in SSP5-8.5.

3.10 Changes to ecosystem services under climate change scenarios

Eight ecosystem services were assessed in this study, as shown in the list below. These services were chosen as they are important to the people living in and visiting the MPA. The two supporting ecosystem services were primary production and formation of habitats. These services contribute to the provisioning and regulating services. For example, habitat formation is important for young fish and primary production creates biomass to ensure fish stocks. The regulating service, climate regulation, reduces the effects of climate change globally by drawing down carbon dioxide and other greenhouse gases out of the atmosphere. This will continue to remain a crucial marine ecosystem service in the future as it can contribute to the sequestration of excess greenhouse gases. Regulation of water and sediment quality is important for fish stocks but also for the recreation, education and scientific research, which takes place around the MPA. The MPA is a no-take MPA but the potential to provide fish and shellfish for food for human consumption is still crucial, because either regulations may change and to allow fish stocks a refuge. Provision of genetic resources can provide resources for scientific research which may be used in the future for medicine and other applications. While Ascension Island is small and not easy to reach, tourists do visit for nature watching. Ascension Island is also used to improve our understanding of marine ecology and in particular of deep sea habitats.

- Supporting Services:
  - Primary production: Production of biomass using solar energy. In the absence of sun light (at ocean depth) biomass is produced through energy gained from inorganic molecules (Armstrong et al., 2012).
  - Formation of habitats: Creation of physical properties of habitats to aid survival of species.
- Regulating Services:
  - Climate regulation: The maintenance of the chemical composition of the atmosphere and oceans to ensure a favourable climate.
  - Regulation of water and sediment quality: Removal of wastes from the water column and sediments.
- Provisioning Services:
  - Fish and shellfish provision: Provision of food from the marine environment
  - Genetic resources: Novel compounds derived from marine species
- Cultural Services:
  - Tourism and nature watching: Recreational activities relying on the marine environment or the biological features of this environment
  - Education and scientific knowledge: Education and science outputs derived from the marine environment

Three habitats were selected for the assessment due to their importance in contributing to ecosystem services around Ascension Island MPA (La Bianca et al., 2018). These were deep sea corals and biogenic reefs; intertidal rocky assemblages and intertidal soft sediments, shown in tab. 5 Their sensitivity to climate change impacts (as modelled here) was assessed based on (La Bianca et al., 2018; Ramirez-Llodra et al., 2011).

The current contribution of each habitat to each of the ecosystem services was adapted from (La Bianca et al., 2018). The habitat types listed in their study were reduced to biogenic and deep sea corals. The current contribution of each habitat to each of the selected habitats is based on (Armstrong et al., 2012; La Bianca et al., 2018)

The last assessment step was used to link the ecosystem services assessment with the CMIP6 data provided here to provide estimate a future trend of the ecosystem service provision 6. Due to the sensitivity of the deep sea biogenic reefs and corals, the trend of most ecosystem services is expected to be reduced. Chemosynthetic primary production is the only service thought not to be affected because the modelled data is not showing changes to the situation of the deep sea habitat. The intertidal rocky assemblages

Table 5. Sensitivity of three key service providing habitats to climate change effects. Impact displayed as NE = No evidence, low, NS = not sensitive, Moderate based on (La Bianca et al., 2018; Ramirez-Llodra et al., 2011). Data for intertidal habitats was not given for all pressures. Those with "?" are based on expert opinion.

	Deep sea corals & Biogenic reefs	Intertidal rocky assemblages	Intertidal sand & muddy assemblages
Warmer	Minor impact	Moderate?	Moderate?
More saline	NE	Moderate	Low
Lower pH	Moderate impact	NS?	NS?
Reduced nutrients	NE	Moderate?	Low?
Reduced chlorophyll	NE	NS?	Low?
Reduced Primary Production	NE	Low?	Low?

Table 6. The current contribution of each of three habitats to eight ecosystem services, based on (La Bianca et al., 2018). Contribution level displayed as 3 s̄ignificant contribution, 2 m̄oderate contribution, 1 l̄ow contribution, NE N̄o evidence. Future trends are based on expert opinion of the authors and are displayed as: ↓ = reduction in ecosystem service provision, ⟷ = no changes, NA = not assessed. Note that no data here showed increasing ecosystem service provision Data for intertidal habitats was not given for all pressures. [a] Chemosynthetic production in Deep sea coral and biogenic reefs is used for Primary Production.

Service name	Deep sea coral & biogenic reefs	Future trend	Intertidal rocky assemblages	Future trend	Intertidal sand & muddy assemblages	Future trend
Primary production	3 [a]	⟷	3	↓	3	⟷
Formation of habitats	3	↓	3	↓	3	⟷
Climate regulation	2	↓	1	↓	1	⟷
Regulation of water and sediment quality	2	↓	NE	NA	NE	NA
Fish and shellfish provision	2	↓	2	↓	2	⟷
Genetic resources	3	↓	NE	NA	NE	NA
Tourism &	3	↓	1	↓	3	⟷
nature watching						⟷
Education &	3	↓	1	↓	1	⟷
scientific knowledge						⟷

are also expected to show reduced capacity to provide ecosystem services. This is so because increased temperature, higher salinity and lower primary production are considered to have a moderate impact on this habitat and assemblages. Two services could not be assessed due to lack of evidence: regulation of water and sediment quality and genetic resources. Intertidal muddy and sandy habitats are not expected to have any changes to ecosystem service provision and two services could not be assessed due to lack of evidence (regulation of water and sediment quality and provision of genetic resources).

4 Discussion

The CMIP6 data projects that the MPA region will become warmer, more saline, more acidic, with less nutrients in the mixed layer, and likely to have less chlorophyll and less primary production over the coming century, as summarised in fig. 2. In most cases, these changes are more extreme in the future scenarios that include stronger emission of greenhouse gases and more significant climate change.

These results suggest that the response of the MPA region to climate change will follow the traditional paradigm of open ocean regions: the increase in radiative forcing (heat) from the atmosphere will warm the ocean and increase surface evaporation. This will cause an increase in salinity and stratification, resulting in a shallower mixed layer depth. The forecast decline in the Atlantic Equatorial Undercurrent reflects an overall weakening in the wider Atlantic and local current systems (Richter & Tokinaga, 2022; Eyring et al., 2021) meaning that less water is being transported into the region at any given time. With a shallower mixed layer depth and less transverse currents, there is less mixing of deep nutrient rich water, and the average nutrients concentration at the surface is decreased. With less nutrients available in the well-lit surface layers, the primary production drops, as does the chlorophyll concentration. While it is not investigated here, a similar drop in secondary marine production is also likely. Furthermore, ocean acidification, caused by a higher concentration of atmospheric carbon dioxide being absorbed by the surface layers, is likely to add further stress to marine organisms.

Our analysis of the evolution of the AEU flow indicates a possible substantial weakening of the current, depending on the scenario. In the scenario that shows the most intense weakening (SSP5-8.5), the bulk of change happens in the second half of the century. In the other scenarios, the rate of change is relatively consistent throughout the century . This may be an element of concern as the AEU is responsible for bringing oxygenated surface water to the tropical subsurface layer (Duteil et al., 2014; Hahn et al., 2017; Oschlies et al., 2018) and its variability has been linked to cycles of compression and expansion of the habitat of tropical pelagic fish (Stramma et al., 2012).

Decadal and multi-decadal variations in oxygen concentration in the tropical Atlantic are well documented and are thought to mainly result from the variability in currents redistributing oxygen (Brandt et al., 2015) (Montes et al., 2016). Much of this variability is natural and linked to climatic cycles. The natural portion of the variability can be substantial to the point of obscuring the climate change signal if too short observation periods are considered. This is demonstrated by the comparison of AEU observational flow time series with our multi-model mean. Nevertheless, all projections consistently point at a reduction of the mean AEU flow, this will still be superimposed its natural variability.

Oxygen Minimum Zones (OMZ) are regions where the oxygen concentration drops below 80 mmol m^{-3}. OMZs are generally unsuitable habitat for active, high-metabolic-rate pelagic fishes (Stramma et al., 2012). While several models are already below the OMZ cut off value at 500m in the historical simulations, this behaviour is not seen in the observational dataset. Those models that best match the observational data project a decline in the annual mean oxygen concentration at 500m, but the decline does not approach the OMZ cut-off value of 80 mmol m^{-3}, therefore, it is unlikely that the Marine Protected Area will develop an OMZ.

Many of the fields included here do not show a significant divergence between scenarios in the 2040-2050 decade in this region. This is a direct consequence of the choices defined in the scenario forcing which reflects the inertia and complexity of changing the global socio-economic systems over the next three decades. The second half of the century shows a much wider range of behaviours, and several fields show significant divergences between scenarios after 2050. This is especially true for the multi-model mean surface temperature, salinity and pH.

The effects of climate change as modelled here are likely to affect some habitats and species negatively. This will lead to negative outcomes for some ecosystem services. It is currently difficult to assess these impacts quantitatively due to lack of more detailed information which is why here we considered trends to project ecosystem service delivery in the future. Previous work has suggested that habitat suitability in the Ascension MPA for some tropical tuna species may increase under future climate change (Townhill et al., 2021). However, that analysis was based on expansion of environmental niches defined by sea surface temperature and salinity only. Other projected changes described here, notably increased stratification and decreased productivity, may result in less favourable foraging conditions for large predators.

The model outputs were helpful though to update current understanding of deep sea habitat sensitivities. The work of (La Bianca et al., 2018) have based their climate change pressure data on one key paper (Ramirez-Llodra et al., 2011) and they predicted an expansion of oxygen minimum zones due to climate change. Modelled data here shows that this may not affect the MPA much, which will be vital to keep deep sea habitats and assemblages intact locally and thereby aid ecosystem service provision. (La Bianca et al., 2018) also assessed both reduced and increased salinity. Model outputs for Ascension Island show that the salinity will be increased therefore this would be the only pressure to assess in a further study.

The analysis presented here has a few limitations that can be categorised into methodological limitations, model and data limitations and scientific limitations. When focusing on the ensemble mean, some of the variability is necessarily lost and the trends tend to be smoother. However, what is lost in variability is usually gained in robustness, as the ensemble mean includes information from multiple models. This effect can be seen especially in the oxygen, integrated primary production and chlorophyll figures. An individual models may show a large rise or fall, but the range of the inter-model variability overwhelms the behaviour of individual models. In some cases, a single model with a substantial change can overwhelm the consensus of the other models, for instance in the chlorophyll analysis.

CMIP6 models typically have a resolution around 1 degree by 1 degree. As such, the Ascension Island MPA is typically only represented by a small number of model pixels. This can be as little as 6x6 or 7x7 pixels in the models native resolutions. This means that the MPA is poorly spatially resolved in CMIP6 and that we are unable to use this model to investigate the spatial variability within the MPA. In addition, Ascension Island itself can not be represented in these models, so they can not accurately capture local sub-grid-scale circulation patterns. As shown in tab. 3, the number of models and ensemble members varies significantly between analyses and scenarios. Future studies could objectively judge models according to their historical performance and use this information to weight the final mean (Brunner et al., 2020). Alternatively, looking at each model's internal structure and design decisions could help with subjective judgements of model performance. For instance, future studies may choose to focus only on models that have sufficiently complex marine biogeochemistry models.

The analysis was limited to the data that was available on JASMIN through its connection to BADC at the time that the analysis were performed. This may not include all data from all CMIP6 models. In addition, several models whose data was present were not accessible due to technical problems, such as non-standard formatting or missing years. Similarly, observational datasets were limited by the scarcity of the observational record in the region. While every effort was made to maximise datasets, it may be possible to include additional models, if the data were to become available on JASMIN or elsewhere.

The data available for ecosystem service analysis and sensitivity analysis was limited. Similarly, there was insufficient data available for a full sensitivity analysis of all habitats. However, the assessment (La Bianca et al., 2018) was useful to derive information needed to carry out this work. Further refinements could include assessing intertidal habitats and ecosystem services more thoroughly. Further work could also include modelling ecosystem service provision under climate change using and modelling indicator outputs (Queirós et al., 2021). but this would need another set of modelling approaches in addition to work carried out here.

Within the real-world (as opposed to the modelled) Ascension Island MPA, commercial fishing was halted in 2019. However, the authors are not aware of any CMIP6 model that explicitly include either fish or fishing behaviour. This is in part due to the relative simplicity of the CMIP6 marine biogeochemistry models and the complexity needed to model fisheries. In addition, the format and forcing for ScenarioMIP was decided in 2015, several years before the MPA was created. This means that any positive or negative feedbacks that may occur due to the existence of the MPA will not be included in this analysis. However, these feedbacks are unlikely to fully offset the climate induced pressures described here (Bates et al., 2019). Future work should focus on predicting ecological impacts of changes described here including plankton and nekton biomass and emergent properties such as phytoplankton community structure, stoichiometry or the Carbon to Chlorophyll ratio (de Mora et al., 2016).

One aspect that this study highlighted was the significant divergence between marine biogeochemistry models in CMIP6 in this region. CMIP6 was not designed to study the marine ecosystem in great depth, and as such the range of models is fairly limited to relatively simple and moderate complexity models. A bespoke high-resolution model of the region using a state-of-the-art complexity marine ecosystem model, such as ERSEM (Butenschön et al., 2016; Vichi et al., 2015), would allow a more in-depth analysis of the behaviour in the MPA. Similarly, a 1D water column model could be generated for the MPA at lower cost, but use a more complex marine biogeochemical model. Alternatively, it could be possible to use CMIP6 data to drive an offline fish model for the MPA (Tittensor et al., 2018).

5 Conclusions

An analysis of the CMIP6 forecast for the Ascension Island MPA was presented for the historic period and several future scenarios. The MPA region is forecast to become warmer, more saline, more acidic, with less pelagic nutrients, less chlorophyll and less primary production. In most cases, these changes are more extreme in the future scenarios that are associated with the stronger emission of greenhouse gases. However, even in the most sustainable projections, there is still evidence that these changes will likely occur. Most of the multi-model ensemble mean future projections do not diverge significantly before the year 2050 in this region, but the direction of travel in the year 2050 is significant and can point to a wide range of different climate futures in the second half of the century.

While protected status can shield local ecosystems from fishing and mineral extraction, MPAs will always remain vulnerable to the impacts of climate change. Even in protected regions, these external forces can fundamentally alter the physical, chemical and ecological systems that the MPAs were created to protect. This in turn can lead to reduced ecosystem service provision, impacting not only the marine ecosystem but also the local human population.

A full climate impact assessment for biodiversity in the Ascension MPA was beyond the scope of this study, and many of the necessary biological data do not currently exist. Future work should focus on predicting climate change responses for a wider range of species and habitats, using CMIP6 model outputs summarized here and included in the Supporting Online Material.

6 Open Research

The tools used to perform this analysis are available through the ESMValTool github service. The bulk properties analysis was performed using the ESMValTool recipes, which can be found in the ASCENSION_ISLAND_MPA_FORECAST branch `https://github.com/ESMValGroup/ESMValTool/tree/ascension_island_mpa_forecast`

The data generated through this report is available in netCDF and csv formats. The bulk fields time series and are included as individual ensemble member csv files. The multi-model mean profile data are available as csv files and each multi-model ensemble mean 2D map is included as a separate netCDF file. The AEU data is available as netCDF files containing multi-model mean, standard deviation, minimum and maximum for yearly and monthly average flow values as well as yearly vertical velocity profile at the equator and full velocity field at 23° E, between 3° S and 3° N and between the surface and 500m depth.

Acknowledgments
This work was funded by the UK Darwin Initiative through project DPLUS113 (CRACAB: Climate Resilience and Conservation of Ascension Biodiversity) and by the UKRI natural Environment Research Council, via the TerraFIRMA: Future Impacts, Risks and Mitigation Actions in a changing Earth system project, Grant reference NE/W004895/1. The work of SB has been funded from the European Union's Horizon 2020 research and innovation programme under grant agreement No 869300 FutureMARES. We acknowledge use of the JASMIN data processing facility, a collaborative facility supplied by the Centre for Environmental Data Analysis (CEDA) to support the data analysis requirements of the UK and European climate and Earth system modelling community, and we would like to thank the JASMIN and CEDA teams for their support. We also acknowledge use of the ESMValTool software toolkit and were grateful for their support in developing this work.

References

Armstrong, C. W., Foley, N. S., Tinch, R., & van den Hove, S. (2012). Services from the deep: Steps towards valuation of deep sea goods and services. *Ecosystem Services*, *2*, 2-13. Retrieved from `https://www.sciencedirect.com/science/article/pii/S221204161200006X` doi: https://doi.org/10.1016/j.ecoser.2012.07.001

Barnes, D. K. A., Sands, C. J., Richardson, A., & Smith, N. (2019). Extremes in benthic ecosystem services; blue carbon natural capital shallower than 1000 m in isolated, small, and young ascension island's eez. *Frontiers in Marine Science*, *6*. Retrieved from `https://www.frontiersin.org/articles/10.3389/fmars.2019.00663` doi: 10.3389/fmars.2019.00663

Bates, A. E., Cooke, R. S., Duncan, M. I., Edgar, G. J., Bruno, J. F., Benedetti-Cecchi, L., … Stuart-Smith, R. D. (2019). Climate resilience in marine protected areas and the 'protection paradox'. *Biological Conservation*, *236*, 305-314. Retrieved from `https://www.sciencedirect.com/science/article/pii/S0006320718308346` doi: https://doi.org/10.1016/j.biocon.2019.05.005

Behrenfeld, M. J. (1997). A comsumer's guide to phytoplankton primary productivity models. *Limnology and Oceanography*, *42*(7), 1479–1491.

Bourlès, B., Araujo, M., McPhaden, M. J., Brandt, P., Foltz, G. R., Lumpkin, R., … Perez, R. C. (2019). Pirata: A sustained observing system for tropical atlantic climate research and forecasting. *Earth and Space Science*, *6*(4), 577-616. Retrieved from `https://agupubs.onlinelibrary.wiley.com/doi/abs/10.1029/2018EA000428` doi: https://doi.org/10.1029/2018EA000428

Brandt, P., Bange, H. W., Banyte, D., Dengler, M., Didwischus, S.-H., Fischer, T.,

... Visbeck, M. (2015). Aon the role of circulation and mixing in the ventilation of oxygen minimum zones with a focus on the eastern tropical north atlantic. *Biogeosciences*, *12*, 489–512. Retrieved from https://doi.org/10.5194/bg-12-489-201 doi: https://doi.org/10.5194/bg-12-489-201

Brandt, P., Hahn, J., Schmidtko, S., Tuchen, F. P., Kopte, R., Kiko, R., ... Dengler, M. (2021). Atlantic equatorial undercurrent intensification counteracts warming-induced deoxygenation. *Nature Geoscience*, *14*, 278–282. Retrieved from https://doi.org/10.1038/s41561-021-00716-1 doi: 10.1038/s41561-021-00716-1

Breitburg, D., Levin, L. A., Oschlies, A., Grégoire, M., Chavez, F. P., Conley, D. J., ... Zhang, J. (2018). Declining oxygen in the global ocean and coastal waters. *Science*, *359*(6371), eaam7240. Retrieved from https://www.science.org/doi/abs/10.1126/science.aam7240 doi: 10.1126/science.aam7240

Brunner, L., Pendergrass, A. G., Lehner, F., Merrifield, A. L., Lorenz, R., & Knutti, R. (2020). Reduced global warming from cmip6 projections when weighting models by performance and independence. *Earth System Dynamics*, *11*(4), 995–1012. Retrieved from https://esd.copernicus.org/articles/11/995/2020/ doi: 10.5194/esd-11-995-2020

Bruno, J. F., Bates, A. E., Cacciapaglia, C., Pike, E. P., Amstrup, S. C., van Hooidonk, R., ... Aronson, R. B. (2018, Jun 01). Climate change threatens the world's marine protected areas. *Nature Climate Change*, *8*(6), 499-503. Retrieved from https://doi.org/10.1038/s41558-018-0149-2 doi: 10.1038/s41558-018-0149-2

Butenschön, M., Clark, J., Aldridge, J. N., Allen, J. I., Artioli, Y., Blackford, J., ... Torres, R. (2016). Ersem 15.06: a generic model for marine biogeochemistry and the ecosystem dynamics of the lower trophic levels. *Geoscientific Model Development*, *9*(4), 1293–1339. Retrieved from https://gmd.copernicus.org/articles/9/1293/2016/ doi: 10.5194/gmd-9-1293-2016

Centre of environmental data analysis, jasmin compute machine. (n.d.). Retrieved from https://www.ceda.ac.uk/services/jasmin/

de Boyer Montegut, C., Madec, G., Fischer, A. S., Lazar, A., & Iudicone, D. (2004). Mixed layer depth over the global ocean: An examination of profile data and a profile-based climatology. *Journal of Geophysical Research: Oceans*, *109*(C12). Retrieved from https://agupubs.onlinelibrary.wiley.com/doi/abs/10.1029/2004JC002378 doi: https://doi.org/10.1029/2004JC002378

de Mora, L., Butenschön, M., & Allen, J. I. (2016). The assessment of a global marine ecosystem model on the basis of emergent properties and ecosystem function: a case study with ersem. *Geoscientific Model Development*, *9*(1), 59–76. Retrieved from https://gmd.copernicus.org/articles/9/59/2016/ doi: 10.5194/gmd-9-59-2016

du Pontavice, H., Gascuel, D., Reygondeau, G., Maureaud, A., & Cheung, W. W. L. (2020). Climate change undermines the global functioning of marine food webs. *Global Change Biology*, *26*(3), 1306-1318. Retrieved from https://onlinelibrary.wiley.com/doi/abs/10.1111/gcb.14944 doi: https://doi.org/10.1111/gcb.14944

Duteil, O., Schwarzkopf, F. U., Böning, C. W., & Oschlies, A. (2014). Major role of the equatorial current system in setting oxygen levels in the eastern tropical atlantic ocean: A high-resolution model study. *Geophysical Research Letters*, *41*(6), 2033-2040. Retrieved from https://agupubs.onlinelibrary.wiley.com/doi/abs/10.1002/2013GL058888 doi: https://doi.org/10.1002/2013GL058888

Esmvaltool: A community diagnostic and performance metrics tool for routine evaluation of earth system models in cmip github page. (n.d.). Retrieved from https://github.com/ESMValGroup/ESMValTool

Eyring, V., Bony, S., Meehl, G. A., Senior, C. A., Stevens, B., Stouffer, R. J., & Taylor, K. E. (2016). Overview of the coupled model intercomparison project phase 6 (cmip6) experimental design and organization. *Geoscientific Model Development*, *9*(5), 1937–1958. Retrieved from https://gmd.copernicus.org/articles/9/1937/2016/ doi: 10.5194/gmd-9-1937-2016

Eyring, V., Gillett, N., Achuta Rao, K., Barimalala, R., Barreiro Parrillo, M., Bellouin, N., . . . Sun, Y. (2021). Human influence on the climate system [Book Section]. In V. Masson-Delmotte et al. (Eds.), *Climate change 2021: The physical science basis. contribution of working group i to the sixth assessment report of the intergovernmental panel on climate change* (p. 423–552). Cambridge, United Kingdom and New York, NY, USA: Cambridge University Press. doi: 10.1017/9781009157896.005

Ferraro, R., Waliser, D. E., Gleckler, P., Taylor, K. E., & Eyring, V. (2015). Evolving obs4mips to support phase 6 of the coupled model intercomparison project (cmip6). *Bulletin of the American Meteorological Society*, *96*(8), ES131 - ES133. Retrieved from https://journals.ametsoc.org/view/journals/bams/96/8/bams-d-14-00216.1.xml doi: 10.1175/BAMS-D-14-00216.1

Foltz, G., Brandt, P., Richter, I., Rodríguez-Fonseca, B., Hernandez, F., Dengler, M., . . . Reul, N. (2019). The tropical atlantic observing system. *Front. Mar. Sci*, *6*(206). doi: doi:10.3389/fmars.2019.00206

Fox-Kemper, B., Hewitt, H., Xiao, C., Aoalgeirsdottir, G., Drijfhout, S., Edwards, T., . . . Yu, Y. (2021). Ocean, cryosphere and sea level change [Book Section]. In V. Masson-Delmotte et al. (Eds.), *Climate change 2021: The physical science basis. contribution of working group i to the sixth assessment report of the intergovernmental panel on climate change* (p. 1211–1362). Cambridge, United Kingdom and New York, NY, USA: Cambridge University Press. doi: 10.1017/9781009157896.011

Garcia, H., Weathers, K., Paver, C., Smolyar, I., Boyer, T., Locarnini, M., . . . Reagan, J. (2018a). *World ocean atlas 2018, volume 3: Dissolved oxygen, apparent oxygen utilization, and dissolved oxygen saturation* (Vol. 83; Report). Retrieved from https://archimer.ifremer.fr/doc/00651/76337/

Garcia, H., Weathers, K., Paver, C., Smolyar, I., Boyer, T., Locarnini, M., . . . Reagan, J. (2018b). *World ocean atlas 2018 volume 4: Dissolved inorganic nutrients (phosphate, nitrate and nitrate+nitrite, silicate)* (Vol. 84; Report). Retrieved from https://archimer.ifremer.fr/doc/00651/76337/

Giarolla, E., Siqueira, L. S. P., Bottino, M. J., Malagutti, M., Capistrano, V. B., & Nobre, P. (2015, Jun 01). Equatorial atlantic ocean dynamics in a coupled ocean–atmosphere model simulation. *Ocean Dynamics*, *65*(6), 831-843. Retrieved from https://doi.org/10.1007/s10236-015-0836-8 doi: 10.1007/s10236-015-0836-8

Government, A. I. (2021). *The ascension island marine protected area management plan 2021-26.* (Tech. Rep.). Retrieved from https://www.ascensionmpa.ac/management-plan

Graham, N. A. J., & McClanahan, T. R. (2013, 05). The Last Call for Marine Wilderness? *BioScience*, *63*(5), 397-402. Retrieved from https://doi.org/10.1525/bio.2013.63.5.13 doi: 10.1525/bio.2013.63.5.13

Griffies, S. M., Danabasoglu, G., Durack, P. J., Adcroft, A. J., Balaji, V., Böning, C. W., . . . Yeager, S. G. (2016). Omip contribution to cmip6: experimental and diagnostic protocol for the physical component of the ocean model intercomparison project. *Geoscientific Model Development*, *9*(9), 3231–3296. Retrieved from https://gmd.copernicus.org/articles/9/3231/2016/ doi: 10.5194/gmd-9-3231-2016

Hahn, J., Brandt, P., Schmidtko, S., & Krahmann, G. (2017). Decadal oxygen change in the eastern tropical north atlantic. *Ocean Science*, *13*(4), 551–576. Retrieved from https://os.copernicus.org/articles/13/551/2017/ doi:

10.5194/os-13-551-2017

Hansen, G. J., Ban, N. C., Jones, M. L., Kaufman, L., Panes, H. M., Yasué, M., & Vincent, A. C. (2011). Hindsight in marine protected area selection: A comparison of ecological representation arising from opportunistic and systematic approaches. *Biological Conservation*, *144*(6), 1866-1875. Retrieved from https://www.sciencedirect.com/science/article/pii/S0006320711001236 doi: https://doi.org/10.1016/j.biocon.2011.04.002

Hormann, V., & Brandt, P. (2007). Atlantic equatorial undercurrent and associated cold tongue variability. *Journal of Geophysical Research: Oceans*, *112*(C6). Retrieved from https://agupubs.onlinelibrary.wiley.com/doi/abs/10.1029/2006JC003931 doi: https://doi.org/10.1029/2006JC003931

Jaureguiberry, P., Titeux, N., Wiemers, M., Bowler, D. E., Coscieme, L., Golden, A. S., … Purvis, A. (2022). The direct drivers of recent global anthropogenic biodiversity loss. *Science Advances*, *8*(45), eabm9982. Retrieved from https://www.science.org/doi/abs/10.1126/sciadv.abm9982 doi: 10.1126/sciadv.abm9982

Johns, W., Brandt, P., Bourlès, B., Tantet, A., Papapostolou, A., & Houk, A. (2014). Zonal structure and seasonal variability of the atlantic equatorial undercurrent. *Clim. Dyn.*, *43*, 3047–3069. doi: https://doi.org/10.1007/s00382-014-2136-2

Johns, W. E., Speich, S., Araujo, M., & et. al. (2021). *Tropical atlantic observing system (taos) review report* (Vol. CLIVAR-01/2021; Tech. Rep.). Climate and Ocean - Variability, Predictability, and Change (CLIVAR) Atlantic Region Panel (ARP). doi: https://doi.org/10.36071/clivar.rp.1.2021

Kwiatkowski, L., Torres, O., Bopp, L., Aumont, O., Chamberlain, M., Christian, J. R., … Ziehn, T. (2020). Twenty-first century ocean warming, acidification, deoxygenation, and upper-ocean nutrient and primary production decline from cmip6 model projections. *Biogeosciences*, *17*(13), 3439–3470. Retrieved from https://bg.copernicus.org/articles/17/3439/2020/ doi: 10.5194/bg-17-3439-2020

La Bianca, G., Tillin, H., Hodgson, B., Erni-Cassola, G., Howell, K., & Rees, S. (2018). *Ascension island natural capital assessment: Marine ecosystem services report. natural capital in the uk's overseas territories report series – supplementary report (south atlantic region).* (Tech. Rep.). Joint Nature Conservation Committee (JNCC).

Lee, J.-Y., Marotzke, J., Bala, G., Cao, L., Corti, S., Dunne, J., … Zhou, T. (2021). Future global climate: Scenario-based projections and near-term information [Book Section]. In V. Masson-Delmotte et al. (Eds.), *Climate change 2021: The physical science basis. contribution of working group i to the sixth assessment report of the intergovernmental panel on climate change* (p. 553–672). Cambridge, United Kingdom and New York, NY, USA: Cambridge University Press. doi: 10.1017/9781009157896.006

Locarnini, R. A., Mishonov, A. V., Baranova, O. K., Boyer, T. P., Zweng, M. M., Garcia, H. E., … Smolyar, I. (2018). *World ocean atlas 2018, volume 1: Temperature.* (Vol. 81; Report). Retrieved from https://archimer.ifremer.fr/doc/00651/76337/

Lotze, H. K., Tittensor, D. P., Bryndum-Buchholz, A., Eddy, T. D., Cheung, W. W. L., Galbraith, E. D., … Worm, B. (2019). Global ensemble projections reveal trophic amplification of ocean biomass declines with climate change. *Proceedings of the National Academy of Sciences*, *116*(26), 12907-12912. Retrieved from https://www.pnas.org/doi/abs/10.1073/pnas.1900194116 doi: 10.1073/pnas.1900194116

Maina, G., Osuka, K., & Samoilys, M. (2011, 01). *Opportunities and challenges of community--based marine protected areas in kenya, cordio status report* (Tech. Rep.). Coastal Oceans Research and Development – Indian Ocean (CORDIO)

East Africa.

Montes, E., Muller-Karger, F. E., Cianca, A., Lomas, M. W., Lorenzoni, L., & Habtes, S. (2016). Decadal variability in the oxygeninventory of north atlantic subtropicalunderwater captured by sustained, long-term oceanographic time seriesobservations. *Global Biogeochem. Cycles*, *30*, 460–478. Retrieved from https://doi.org/10.1002/2015GB005183 doi: doi:10.1002/2015GB005183

O'Leary, B. C., Winther-Janson, M., Bainbridge, J. M., Aitken, J., Hawkins, J. P., & Roberts, C. M. (2016). Effective coverage targets for ocean protection. *Conservation Letters*, *9*(6), 398-404. Retrieved from https://conbio.onlinelibrary.wiley.com/doi/abs/10.1111/conl.12247 doi: https://doi.org/10.1111/conl.12247

Olsen, A., Key, R. M., van Heuven, S., Lauvset, S. K., Velo, A., Lin, X., ... Suzuki, T. (2016). The global ocean data analysis project version 2 (glodapv2) – an internally consistent data product for the world ocean. *Earth System Science Data*, *8*(2), 297–323. Retrieved from https://essd.copernicus.org/articles/8/297/2016/ doi: 10.5194/essd-8-297-2016

O'Neill, B. C., Tebaldi, C., van Vuuren, D. P., Eyring, V., Friedlingstein, P., Hurtt, G., ... Sanderson, B. M. (2016). The scenario model intercomparison project (scenariomip) for cmip6. *Geoscientific Model Development*, *9*(9), 3461–3482. Retrieved from https://gmd.copernicus.org/articles/9/3461/2016/ doi: 10.5194/gmd-9-3461-2016

Oschlies, A., Brandt, P., & Stramma, L. (2018). Drivers and mechanisms of ocean deoxygenation. *Nature Geosci*, *11*, 467–473. Retrieved from https://doi.org/10.1038/s41561-018-0152-2 doi: https://doi.org/10.1038/s41561-018-0152-2

O'Regan, S. M., Archer, S. K., Friesen, S. K., & Hunter, K. L. (2021). A global assessment of climate change adaptation in marine protected area management plans. *Frontiers in Marine Science*, *8*. Retrieved from https://www.frontiersin.org/articles/10.3389/fmars.2021.711085 doi: 10.3389/fmars.2021.711085

Poloczanska, E. S., Burrows, M. T., Brown, C. J., García Molinos, J., Halpern, B. S., Hoegh-Guldberg, O., ... Sydeman, W. J. (2016). Responses of marine organisms to climate change across oceans. *Frontiers in Marine Science*, *3*. Retrieved from https://www.frontiersin.org/articles/10.3389/fmars.2016.00062 doi: 10.3389/fmars.2016.00062

Queirós, A. M., Talbot, E., Beaumont, N. J., Somerfield, P. J., Kay, S., Pascoe, C., ... Nic Aonghusa, C. (2021). Bright spots as climate-smart marine spatial planning tools for conservation and blue growth. *Global Change Biology*, *27*(21), 5514-5531. Retrieved from https://onlinelibrary.wiley.com/doi/abs/10.1111/gcb.15827 doi: https://doi.org/10.1111/gcb.15827

Ramirez-Llodra, E., Tyler, P. A., Baker, M. C., Bergstad, O. A., Clark, M. R., Escobar, E., ... Van Dover, C. L. (2011, 08). Man and the last great wilderness: Human impact on the deep sea. *PLOS ONE*, *6*(8), 1-25. Retrieved from https://doi.org/10.1371/journal.pone.0022588 doi: 10.1371/journal.pone.0022588

Riahi, K., van Vuuren, D. P., Kriegler, E., Edmonds, J., O'Neill, B. C., Fujimori, S., ... Tavoni, M. (2017). The shared socioeconomic pathways and their energy, land use, and greenhouse gas emissions implications: An overview. *Global Environmental Change*, *42*, 153-168. Retrieved from https://www.sciencedirect.com/science/article/pii/S0959378016300681 doi: https://doi.org/10.1016/j.gloenvcha.2016.05.009

Richter, I., & Tokinaga, H. (2022). An overview of the performance of cmip6 models in the tropical atlantic: mean state, variability, and remote impacts. *Climate Dynamics*, *55*, 2579–2601. Retrieved from https://doi.org/10.1007/s00382-020-05409-w doi: https://doi.org/10.1007/s00382-020-05409-w

Righi, M., Andela, B., Eyring, V., Lauer, A., Predoi, V., Schlund, M., … Zimmermann, K. (2020). Earth system model evaluation tool (esmvaltool) v2.0 – technical overview. *Geoscientific Model Development*, *13*(3), 1179–1199. Retrieved from `https://gmd.copernicus.org/articles/13/1179/2020/` doi: 10.5194/gmd-13-1179-2020

Sathyendranath, S., Brewin, R. J., Brockmann, C., Brotas, V., Calton, B., Chuprin, A., … Platt, T. (2019). An ocean-colour time series for use in climate studies: The experience of the ocean-colour climate change initiative (oc-cci). *Sensors*, *19*(19). Retrieved from `https://www.mdpi.com/1424-8220/19/19/4285` doi: 10.3390/s19194285

Sellar, A. A., Walton, J., Jones, C. G., Wood, R., Abraham, N. L., Andrejczuk, M., … Griffiths, P. T. (2020). Implementation of u.k. earth system models for cmip6. *Journal of Advances in Modeling Earth Systems*, *12*(4), e2019MS001946. Retrieved from `https://agupubs.onlinelibrary.wiley.com/doi/abs/10.1029/2019MS001946` (e2019MS001946 10.1029/2019MS001946) doi: https://doi.org/10.1029/2019MS001946

Stramma, L., Prince, E. D., Schmidtko, S., Luo, J., Hoolihan, J. P., Visbeck, M., … Körtzinger, A. (2012). Expansion of oxygen minimum zones may reduce available habitat for tropical pelagic fishes. *Nat. Clim. Change*, *2*, 33-37. Retrieved from `https://www.nature.com/articles/nclimate1304` doi: DOI:10.1038/NCLIMATE1304

Sukhdev, P., Wittmer, H., Schröter-Schlaack, C., Nesshöver, C., Bishop, J., ten Brink, P., … Simmons, B. (2010). *The economics of ecosystems and biodiversity: Mainstreaming the economics of nature: A synthesis of the approach, conclusions and recommendations of teeb.* (Tech. Rep.). The Economics of Ecosystems and Biodiversity.

Tittensor, D. P., Beger, M., Boerder, K., Boyce, D. G., Cavanagh, R. D., Cosandey-Godin, A., … Worm, B. (2019). Integrating climate adaptation and biodiversity conservation in the global ocean. *Science Advances*, *5*(11), eaay9969. Retrieved from `https://www.science.org/doi/abs/10.1126/sciadv.aay9969` doi: 10.1126/sciadv.aay9969

Tittensor, D. P., Eddy, T. D., Lotze, H. K., Galbraith, E. D., Cheung, W., Barange, M., … Walker, N. D. (2018). A protocol for the intercomparison of marine fishery and ecosystem models: Fish-mip v1.0. *Geoscientific Model Development*, *11*(4), 1421–1442. Retrieved from `https://gmd.copernicus.org/articles/11/1421/2018/` doi: 10.5194/gmd-11-1421-2018

Tokinaga, H., & Xie, S.-P. (2011, Apr 01). Weakening of the equatorial atlantic cold tongue over the past six decades. *Nature Geoscience*, *4*(4), 222-226. Retrieved from `https://doi.org/10.1038/ngeo1078` doi: 10.1038/ngeo1078

Townhill, B. L., Couce, E., Bell, J., Reeves, S., & Yates, O. (2021). Climate change impacts on atlantic oceanic island tuna fisheries. *Frontiers in Marine Science*, *8*. Retrieved from `https://www.frontiersin.org/articles/10.3389/fmars.2021.634280` doi: 10.3389/fmars.2021.634280

Vichi, M., Lovato, T., Lazzari, P., Cossarini, G., Gutierrez Mlot, E., Mattia, G., … Zavatarelli, M. (2015, 08). *The biogeochemical flux model (bfm): Equation description and user manual. bfm version 5.1. release 1.1* (Tech. Rep.). doi: 10.13140/RG.2.1.2176.9444

Watson, R. T., & Zakri, A. (2005). *Ecosystems and human well-being: Opportunities and challenges for business and industry* (Tech. Rep.). Millennium Ecosystem Assessment.

Weber, S. B., & Weber, N. (2019, Nov 01). Important bird areas: Ascension island. *British Birds*, *112*(11), 661-682-3018.

Weber, S. B., Weber, N., Ellick, J., Avery, A., Frauenstein, R., Godley, B. J., … Broderick, A. C. (2014, Nov 01). Recovery of the south atlantic's largest green turtle nesting population. *Biodiversity and Conservation*, *23*(12), 3005-

3018. Retrieved from https://doi.org/10.1007/s10531-014-0759-6 doi: 10.1007/s10531-014-0759-6

Weijer, W., Cheng, W., Garuba, O. A., Hu, A., & Nadiga, B. T. (2020). Cmip6 models predict significant 21st century decline of the atlantic meridional overturning circulation. *Geophysical Research Letters*, *47*(12), e2019GL086075. Retrieved from https://agupubs.onlinelibrary.wiley.com/doi/abs/10.1029/2019GL086075 (e2019GL086075 10.1029/2019GL086075) doi: https://doi.org/10.1029/2019GL086075

Wilson, K. L., Tittensor, D. P., Worm, B., & Lotze, H. K. (2020). Incorporating climate change adaptation into marine protected area planning. *Global Change Biology*, *26*(6), 3251-3267. Retrieved from https://onlinelibrary.wiley.com/doi/abs/10.1111/gcb.15094 doi: https://doi.org/10.1111/gcb.15094

Wirtz, P., Bingeman, J., Bingeman, J., Fricke, R., Hook, T. J., & Young, J. (2017). The fishes of ascension island, central atlantic ocean – new records and an annotated checklist. *Journal of the Marine Biological Association of the United Kingdom*, *97*(4), 783–798. doi: 10.1017/S0025315414001301

Woodley, S., Locke, H., Laffoley, D., MacKinnon, K., Sandwith, T., & Smart, J. (2019, 12). A review of evidence for area-based conservation targets for the post-2020 global biodiversity framework. *PARKS*, 31-46. doi: 10.2305/IUCN.CH.2019.PARKS-25-2SW2.en

Zweng, M. M., Reagan, J. R., Seidov, D., Boyer, T. P., Locarnini, R. A., Garcia, H. E., … Smolyar, I. (2018). *World ocean atlas 2018, volume 2: Salinity.* (Vol. 82; Report). Retrieved from https://archimer.ifremer.fr/doc/00651/76337/

Figure 1.

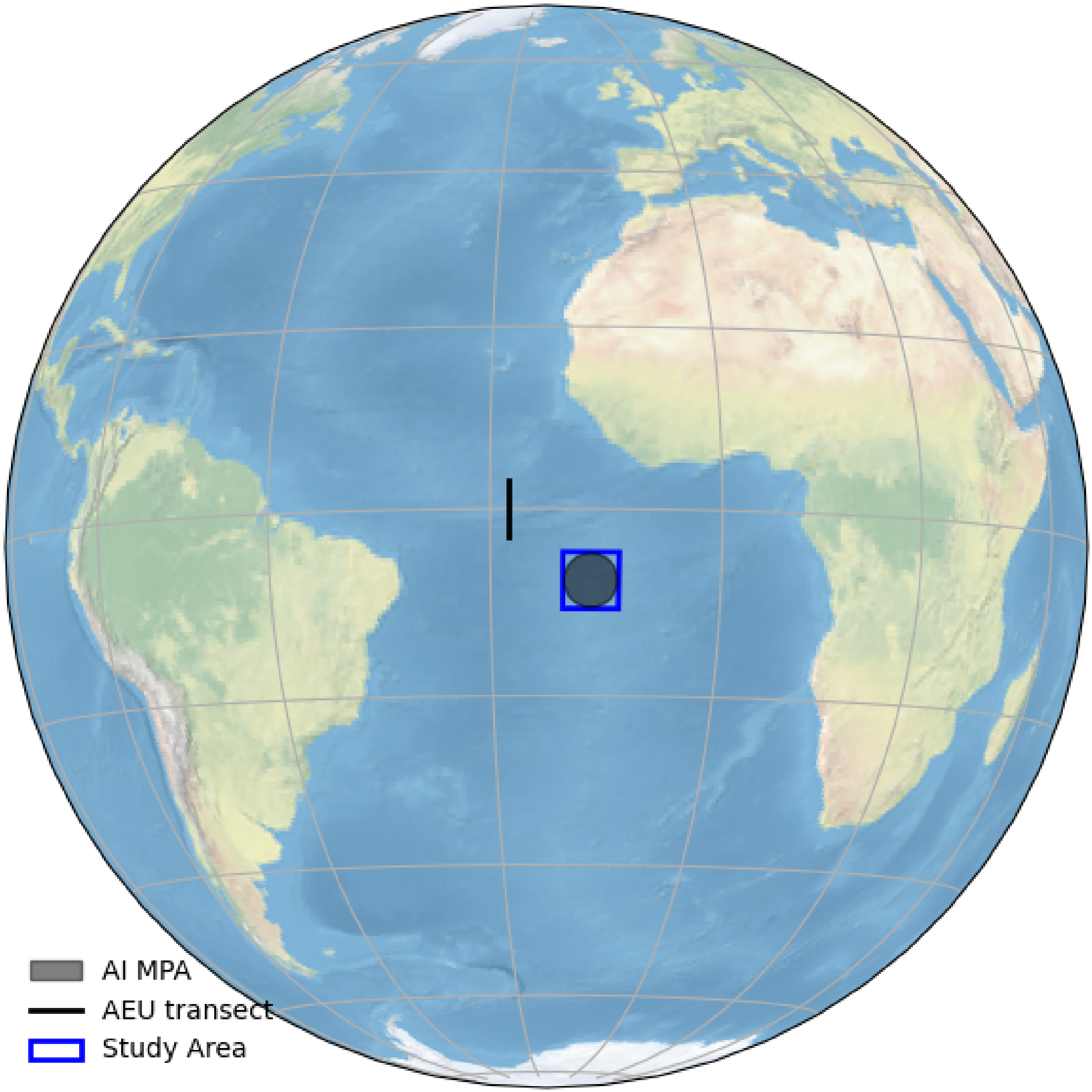
AI MPA
AEU transect
Study Area

Figure 2.

Ascension Island Marine Protected Area Forecast

Forecast for 2040-2050

Anomaly against 2000-2010

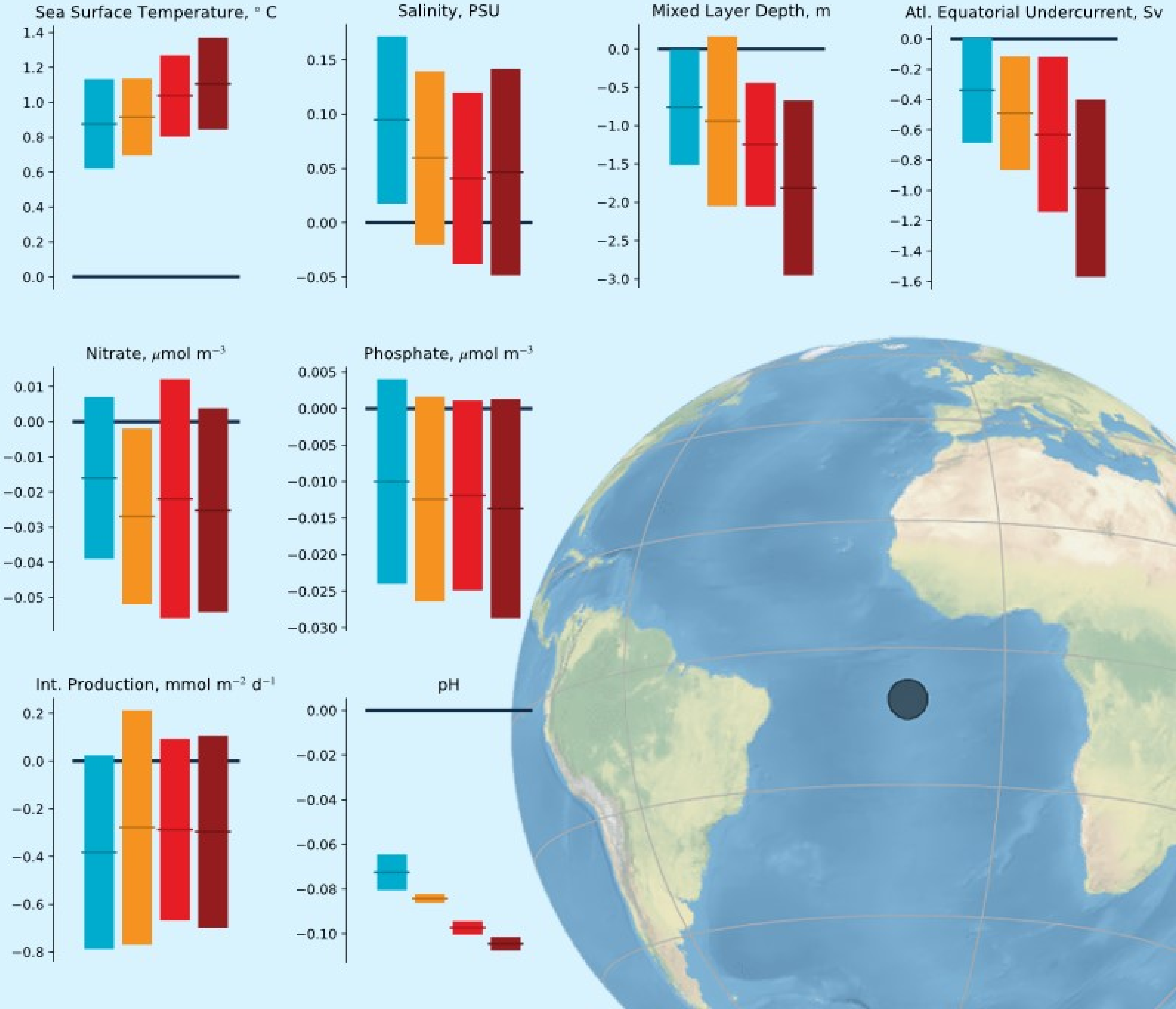

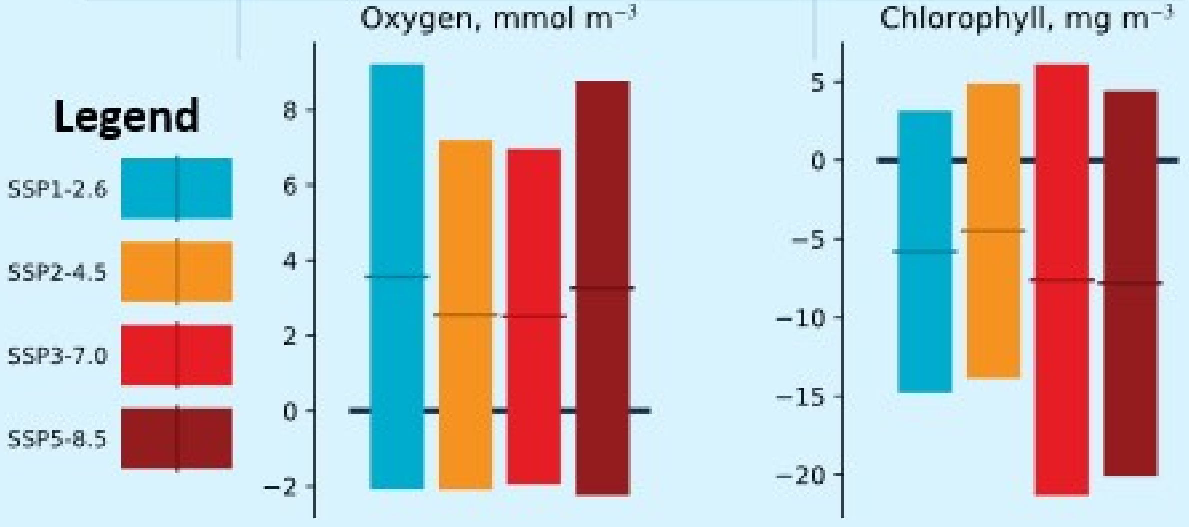

Figure 3.

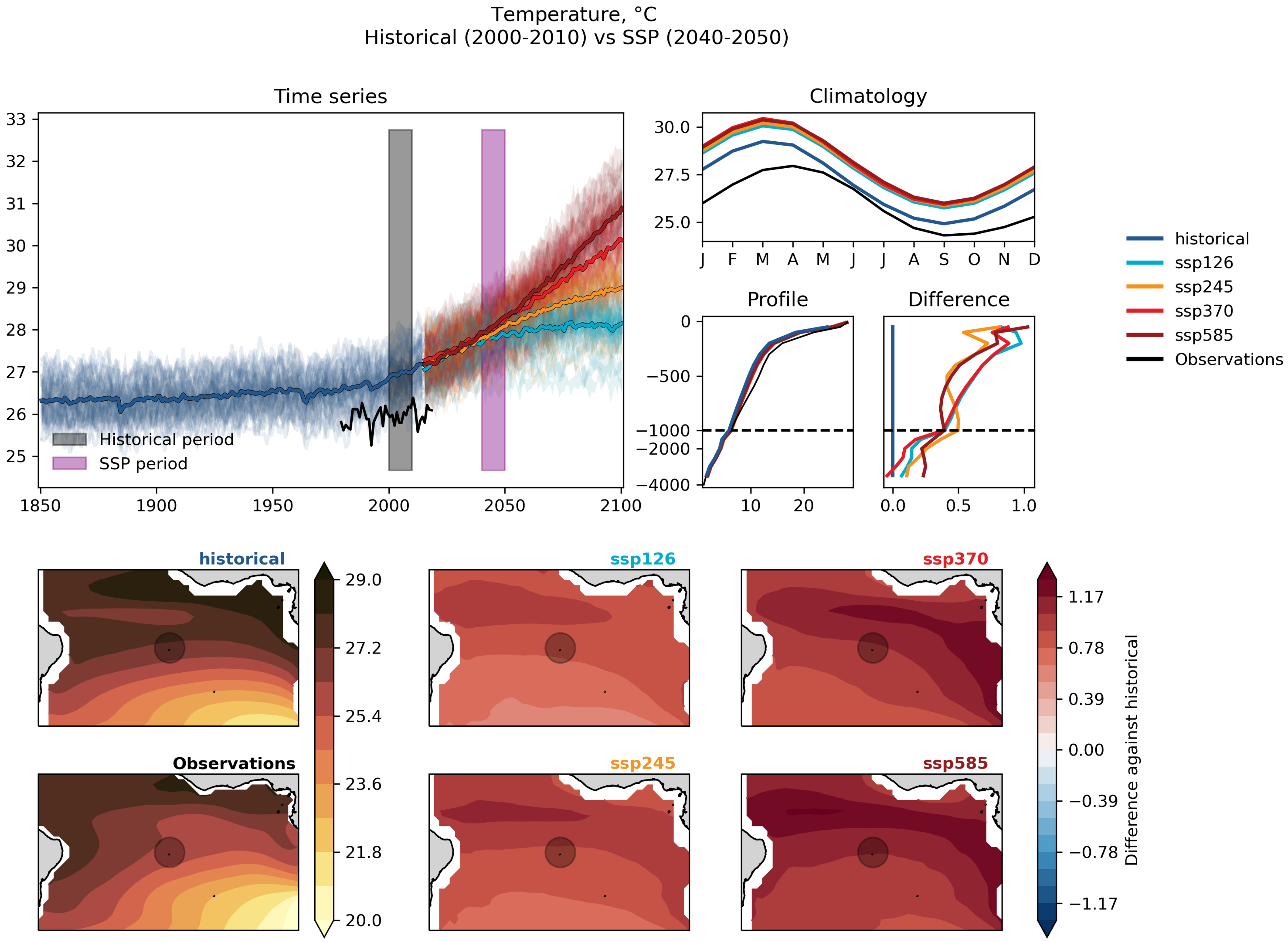
Temperature, °C
Historical (2000-2010) vs SSP (2040-2050)
Time series
Historical period
SSP period
Climatology
J F M A M J J A S O N D
Profile
Difference
historical
ssp126
ssp245
ssp370
ssp585
Observations
historical
Observations
ssp126
ssp370
ssp245
ssp585
29.0
27.2
25.4
23.6
21.8
20.0
1.17
0.78
0.39
0.00
−0.39
−0.78
−1.17
Difference against historical

Figure 4.

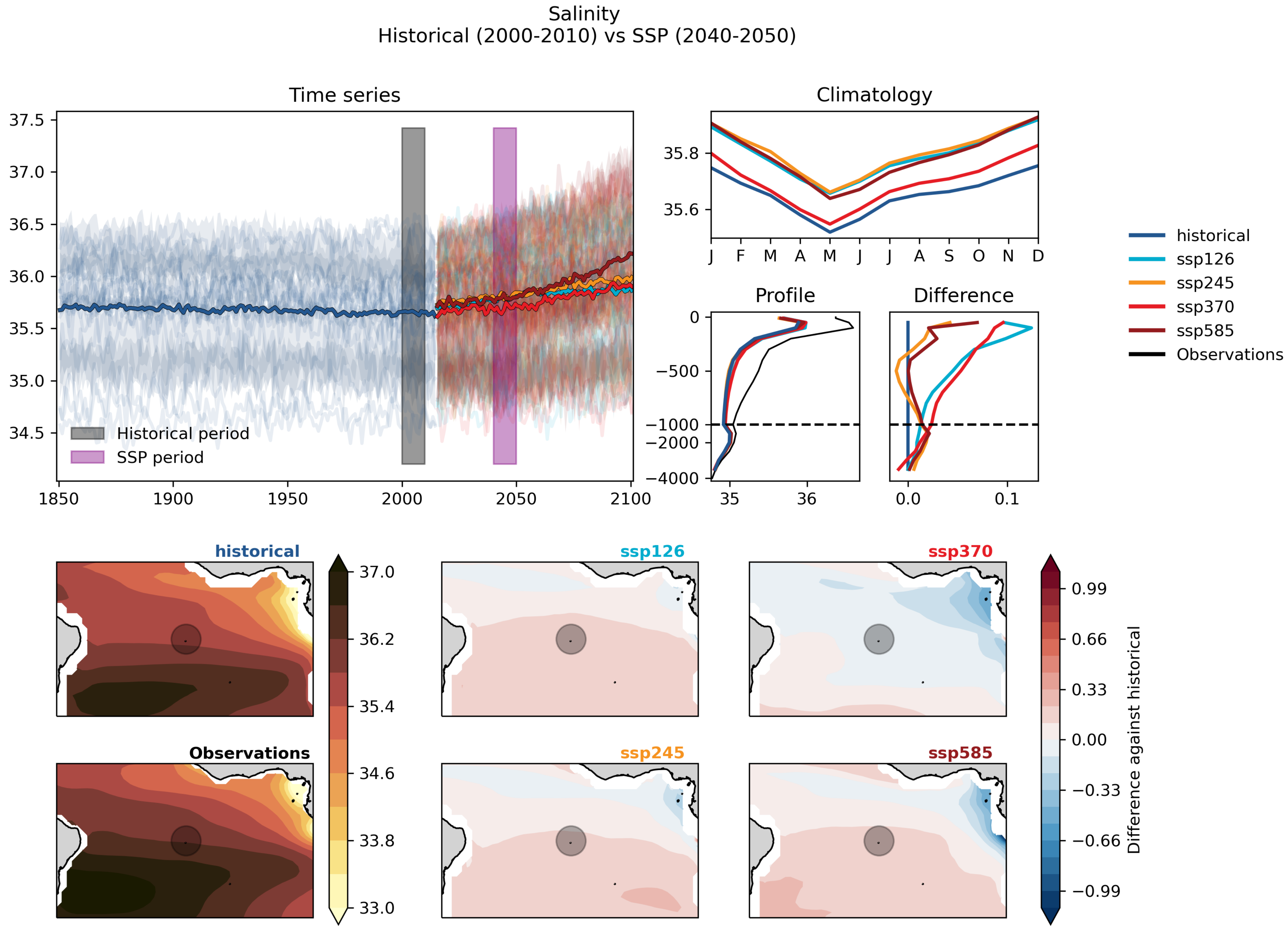
Salinity
Historical (2000-2010) vs SSP (2040-2050)
Time series
Historical period
SSP period
Climatology
Profile
Difference
historical
ssp126
ssp245
ssp370
ssp585
Observations
historical
Observations
ssp126
ssp370
ssp245
ssp585
Difference against historical

Figure 5.

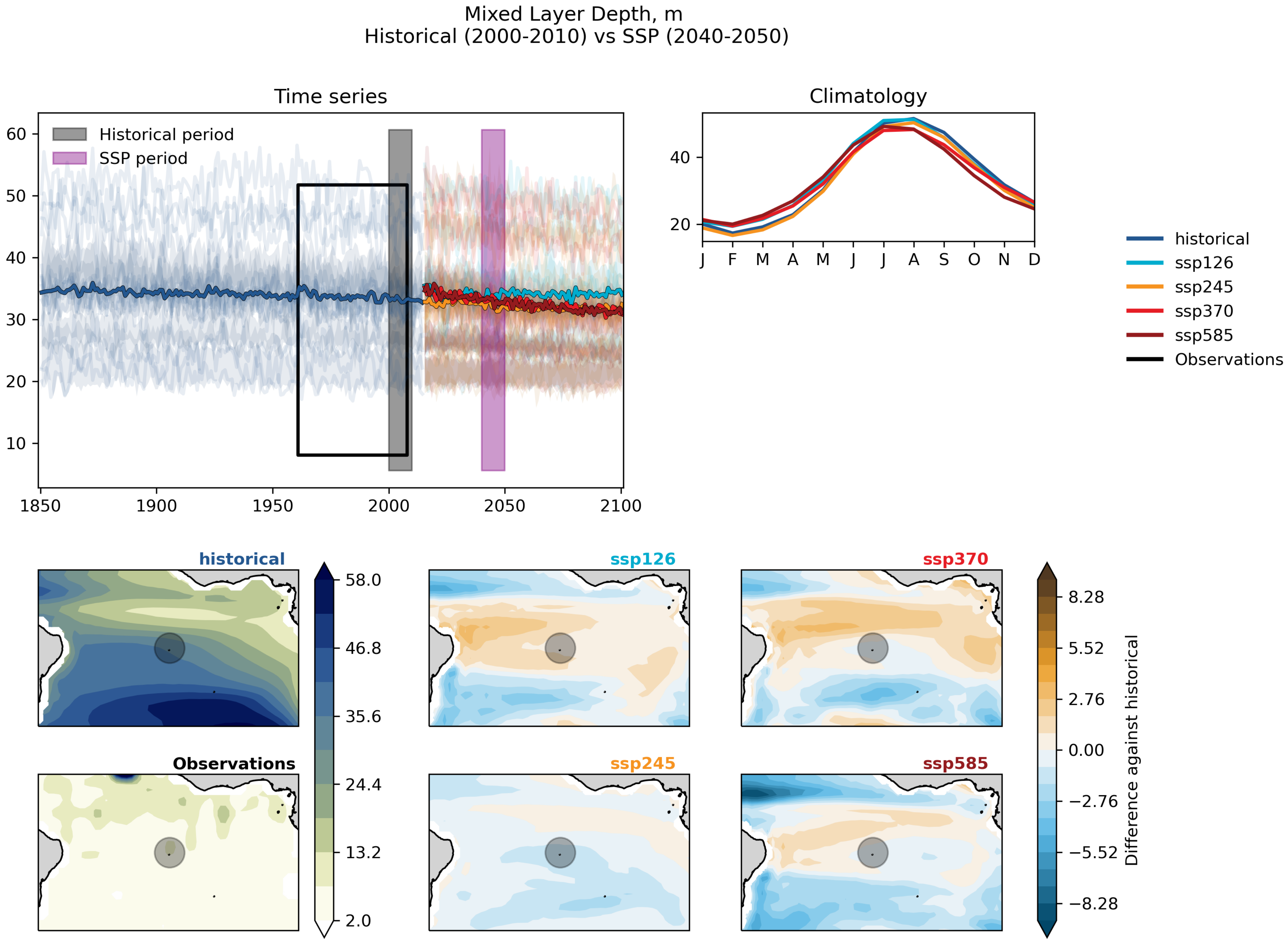
Mixed Layer Depth, m
Historical (2000-2010) vs SSP (2040-2050)
Time series
Historical period
SSP period
60
50
40
30
20
10
1850
1900
1950
2000
2050
2100
Climatology
40
20
J F M A M J J A S O N D
historical
ssp126
ssp245
ssp370
ssp585
Observations
historical
Observations
58.0
46.8
35.6
24.4
13.2
2.0
ssp126
ssp245
ssp370
ssp585
8.28
5.52
2.76
0.00
−2.76
−5.52
−8.28
Difference against historical

Figure 6.

Disolved Oxygen Concentration at 500m, mmol m^{-3}
Historical (2000-2010) vs SSP (2040-2050)

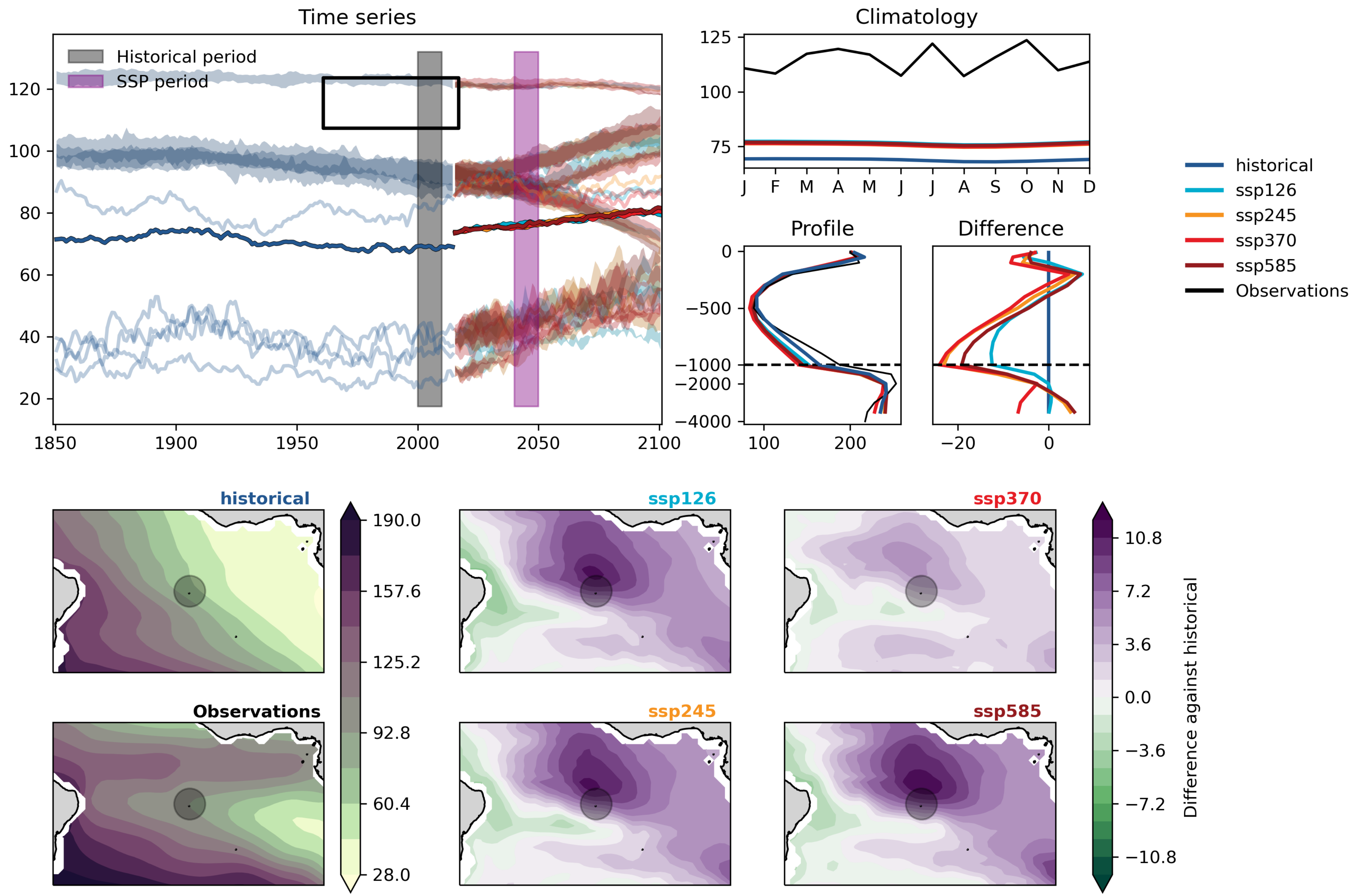

Figure 7.

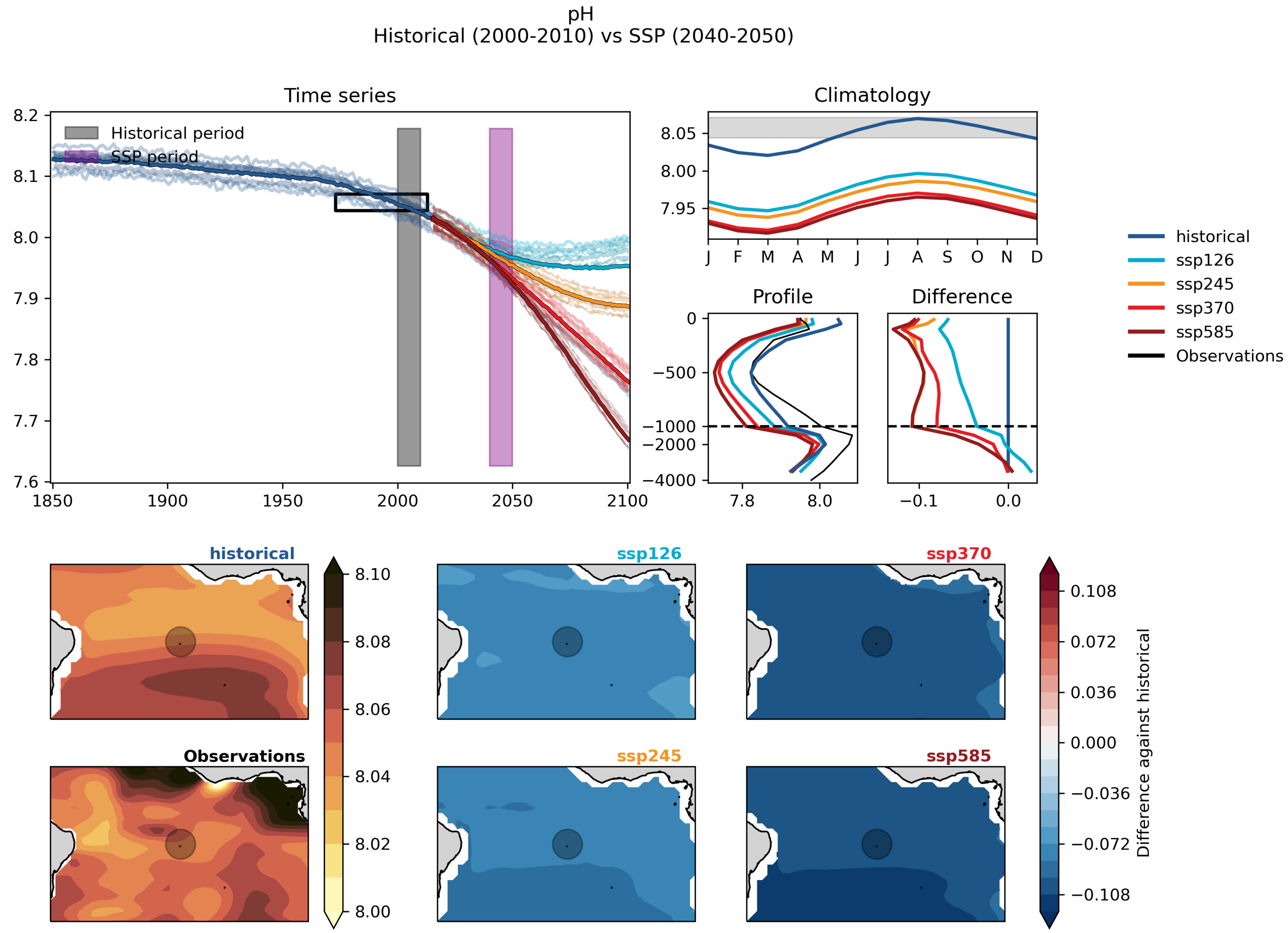

pH
Historical (2000-2010) vs SSP (2040-2050)
Time series
Historical period
SSP period
8.2
8.1
8.0
7.9
7.8
7.7
7.6
1850
1900
1950
2000
2050
2100
Climatology
8.05
8.00
7.95
J F M A M J J A S O N D
Profile
Difference
0
−500
−1000
−2000
−4000
7.8
8.0
−0.1
0.0
historical
ssp126
ssp245
ssp370
ssp585
Observations
historical
Observations
8.10
8.08
8.06
8.04
8.02
8.00
ssp126
ssp245
ssp370
ssp585
0.108
0.072
0.036
0.000
−0.036
−0.072
−0.108
Difference against historical

Figure 8.

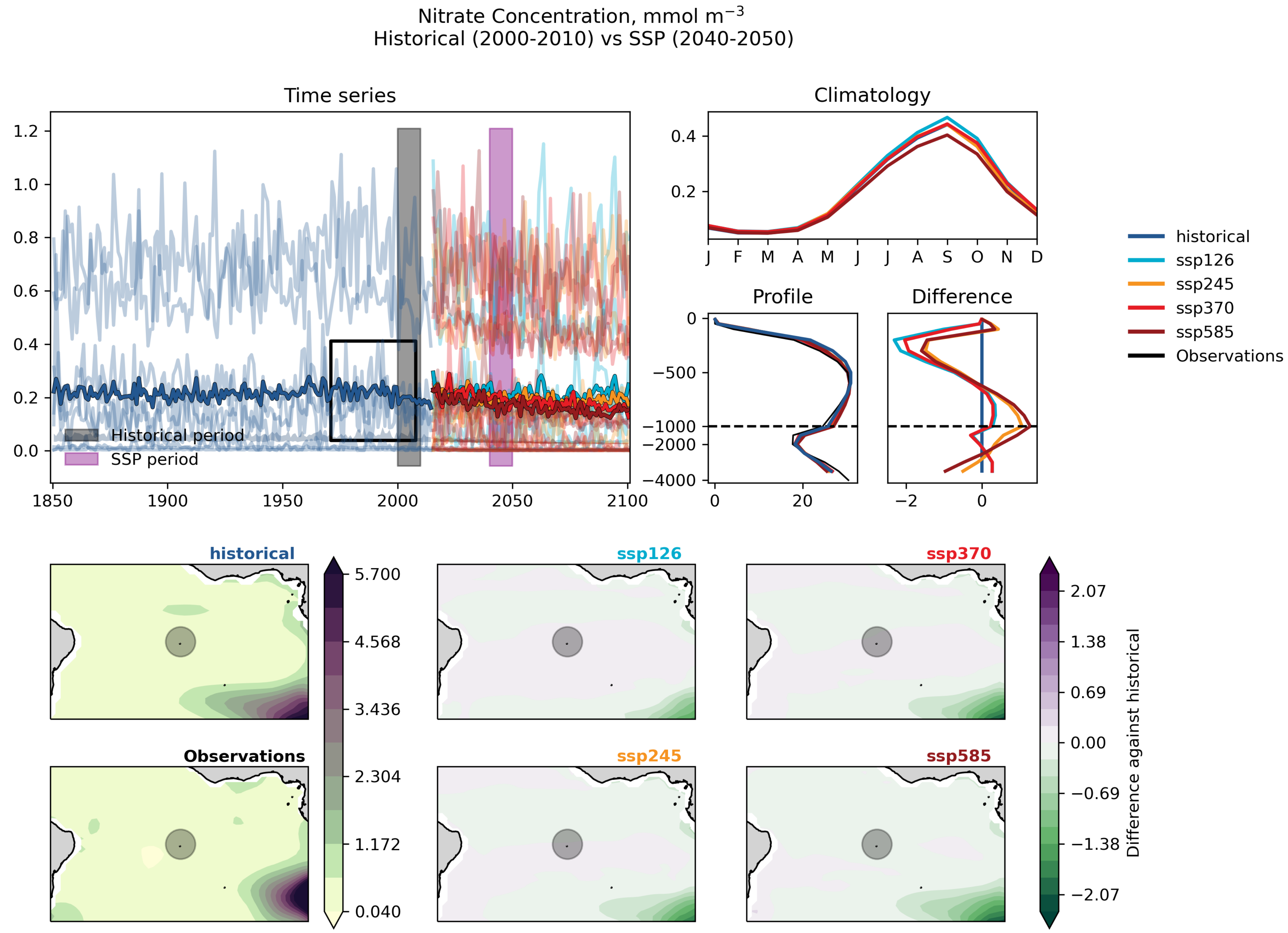

Nitrate Concentration, mmol m^{-3}
Historical (2000-2010) vs SSP (2040-2050)
Time series
Historical period
SSP period
Climatology
Profile
Difference
historical
ssp126
ssp245
ssp370
ssp585
Observations
Difference against historical

Figure 9.

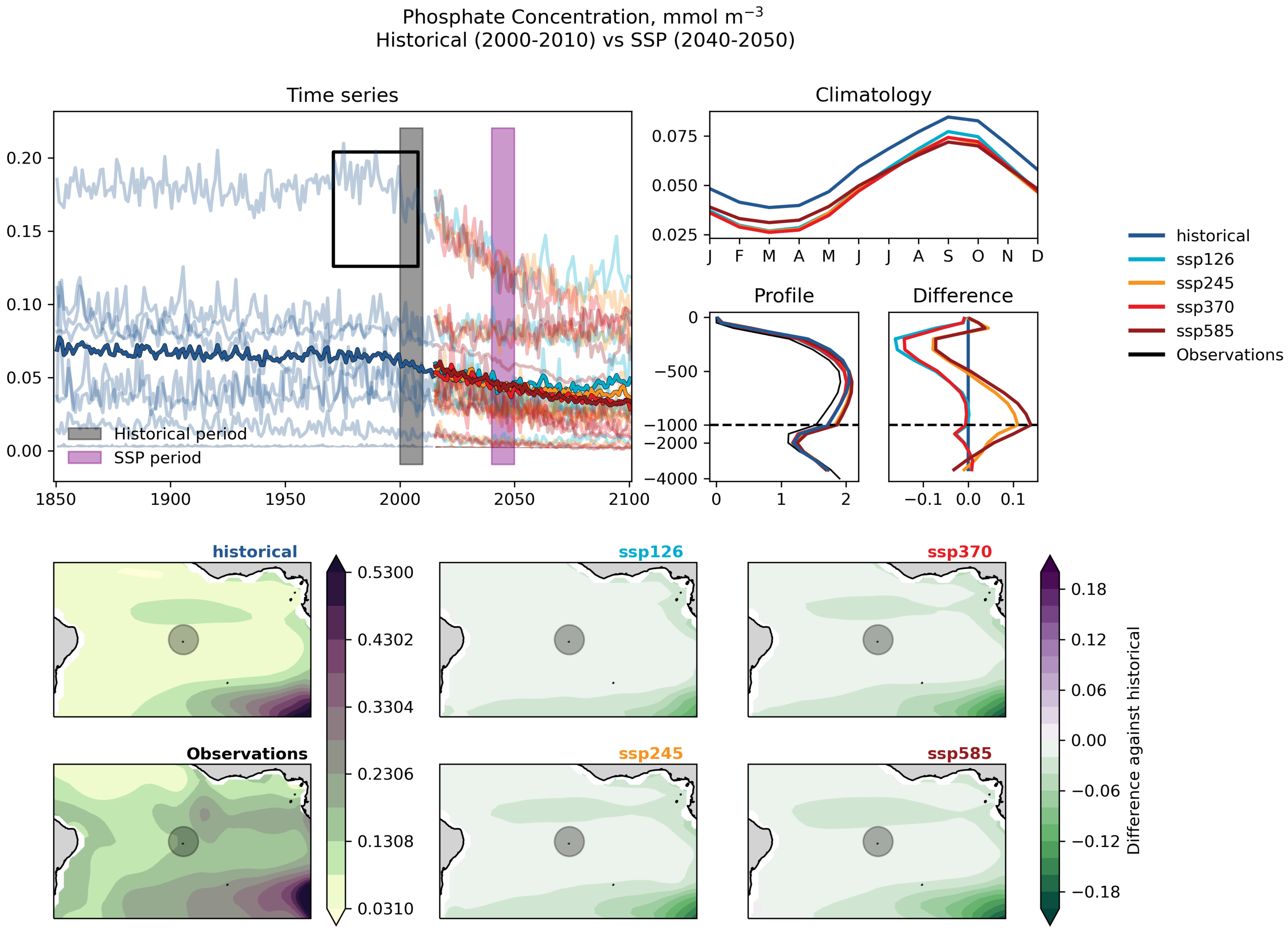

Phosphate Concentration, mmol m^{-3}
Historical (2000-2010) vs SSP (2040-2050)
Time series
Historical period
SSP period
Climatology
J F M A M J J A S O N D
Profile
Difference
historical
ssp126
ssp245
ssp370
ssp585
Observations
historical
ssp126
ssp370
Observations
ssp245
ssp585
0.5300
0.4302
0.3304
0.2306
0.1308
0.0310
Difference against historical

Figure 10.

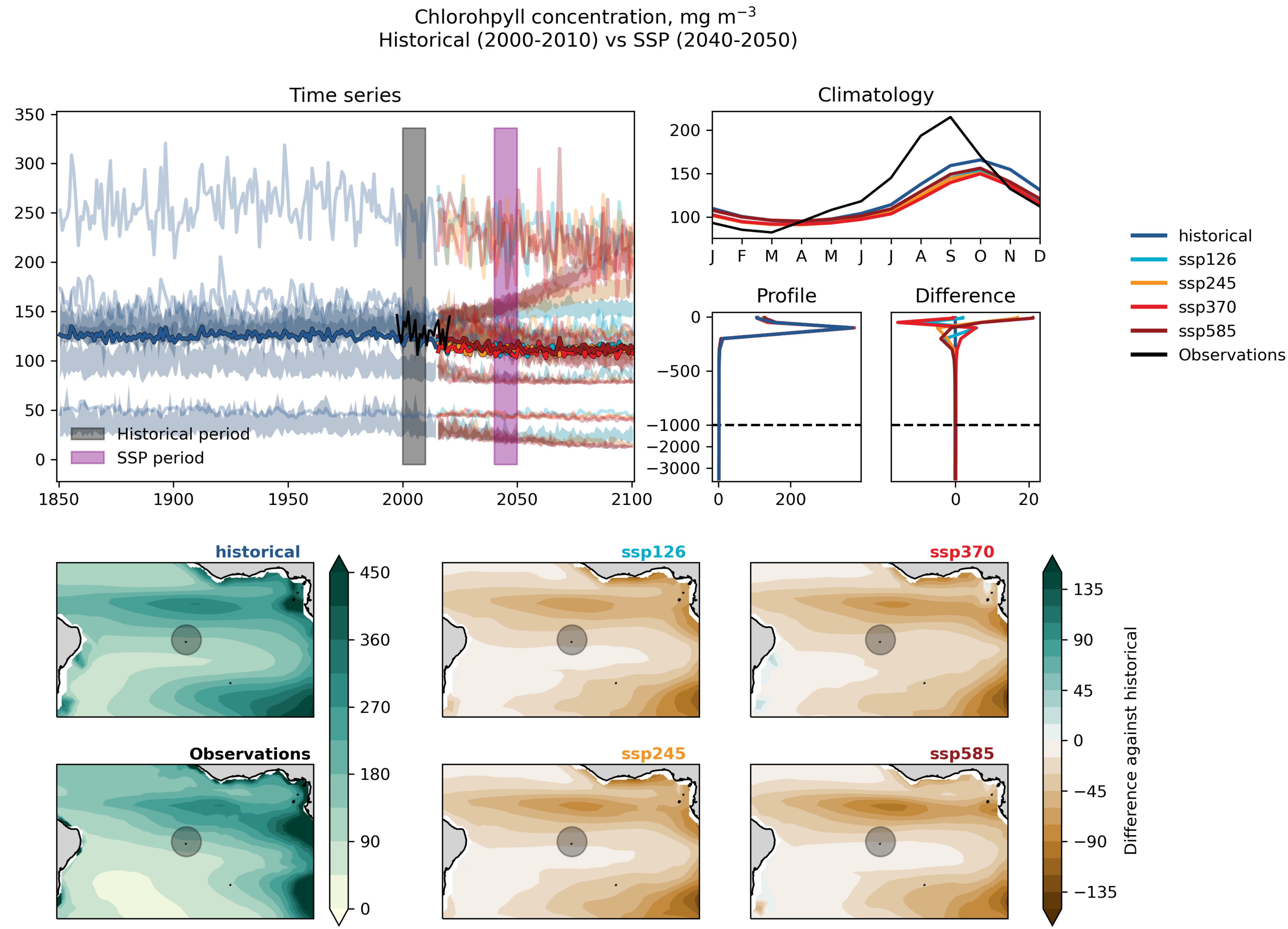

Chlorohpyll concentration, mg m^{-3}
Historical (2000-2010) vs SSP (2040-2050)
Time series
Historical period
SSP period
Climatology
J F M A M J J A S O N D
Profile
Difference
historical
ssp126
ssp245
ssp370
ssp585
Observations
historical
Observations
ssp126
ssp370
ssp245
ssp585
Difference against historical

Figure 11.

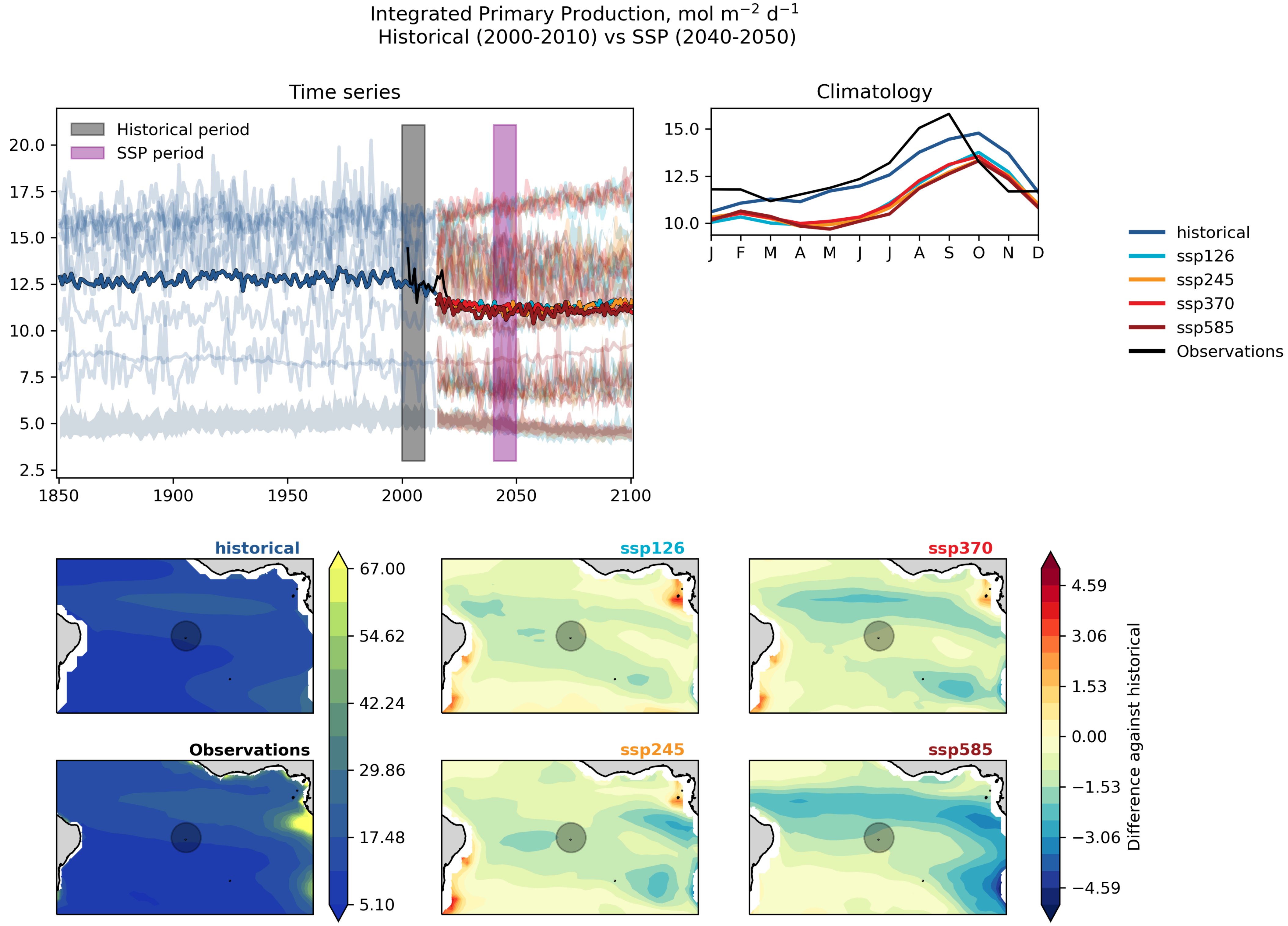
Integrated Primary Production, mol m^{-2} d^{-1}
Historical (2000-2010) vs SSP (2040-2050)
Time series
Historical period
SSP period
20.0
17.5
15.0
12.5
10.0
7.5
5.0
2.5
1850
1900
1950
2000
2050
2100
Climatology
15.0
12.5
10.0
J F M A M J J A S O N D
historical
ssp126
ssp245
ssp370
ssp585
Observations
historical
Observations
67.00
54.62
42.24
29.86
17.48
5.10
ssp126
ssp370
ssp245
ssp585
4.59
3.06
1.53
0.00
−1.53
−3.06
−4.59
Difference against historical

Figure 12.

AEU flow
Historical (2000-2010) vs SSP (2040-2050)